Chapter 3
Clinical and Radiologic Features

Anja C. Roden and Christine U. Lee

Introduction

Patients with diffuse malignant pleural mesothelioma often have an insidious onset of symptoms. Nonspecific symptoms may be present for several months and even years until a diagnosis is rendered. At that time, many of the symptoms reflect advanced disease with signs of progressive local expansion of the tumor, tumor invasion into surrounding structures, and/or tumor spread. A combination of patient symptoms and signs at the time of diagnosis is common (Table 3.1). The two most common symptoms are dyspnea and chest pain which are reported in approximately 90 % of patients [1].

Diffuse Malignant Pleural Mesothelioma: Clinical Signs and Symptoms

Dyspnea

The most common cause of dyspnea in patients with diffuse malignant pleural mesothelioma is a large pleural effusion [2]. Pleural effusion in diffuse malignant pleural mesothelioma is usually unilateral, present at the site of disease. The effusion might cause atelectasis and/or pneumonia of the underlying lung and might restrict

A. C. Roden (✉)
Department of Laboratory Medicine and Pathology, Mayo Clinic,
200 First Street SW, Rochester, MN 55905, USA
e-mail: Roden.anja@mayo.edu

C. U. Lee
Department of Radiology, Mayo Clinic, 200 First Street SW, Rochester, MN, USA

Table 3.1 Signs and symptoms of patients with diffuse malignant pleural mesothelioma

Signs and symptoms	Percent patients
Pulmonary	
Dyspnea [1, 7, 23, 24, 31, 47]	35–82
Pleural effusion [6, 7, 31, 85]	54–87
Chest pain [1, 7, 23, 24, 31, 47, 85]	35–71
Cough [7, 23, 31, 47]	6–37
Increased sputum production [31]	18
Pneumothorax/hydropneumothorax [6, 85]	≤10
Interstitial lung disease [9−13]	≤6
Systemic	
Fatigue [7,31]	18–33
Weight loss [7, 24, 31, 47, 85]	9–59
Anorexia [7]	11
Fever, chills, or sweat [7, 23, 47, 85]	6–33
Pericardial effusions [47]	9
Sensation of heaviness or fullness of chest [7]	7
Hoarseness, early satiety, myalgia [7]	≤3 each
No symptoms, incidental diagnosis [23, 31, 47]	3–8

the movement of the ipsilateral hemidiaphragm. In advanced disease, malignant mesothelioma usually encases the lung resulting in restrictive lung function and/or pneumonia [3].

Patients might present with pneumothorax or hydropneumothorax which usually also results in dyspnea (Fig. 3.1). Once thought to be rare, pneumothorax or hydropneumothorax as initial presentation is now understood to occur in up to 10 % of cases. In a series of 91 patients who underwent pleurectomy for spontaneous pneumothorax, five patients (4.3 %) were diagnosed with malignant mesothelioma [4]. Alkhuja et al. described four patients who presented with spontaneous pneumothorax and were ultimately diagnosed with malignant mesothelioma [5]. Two of the four patients were diagnosed with malignant mesothelioma 12 and 22 months after the initial pneumothorax. Pneumothorax might be under-recognized in this patient population given a recent radiologic study of 92 patients who were diagnosed with malignant pleural mesothelioma between 1997 and 2006 [6]. Nine (of 92) patients (10 %) were found to have pneumothorax on computed tomography (CT) imaging studies.

Dyspnea due to mesothelioma might be compounded by other lung diseases that are often present in this patient population such as chronic obstructive pulmonary disease, asbestosis, or ischemic heart disease [3].
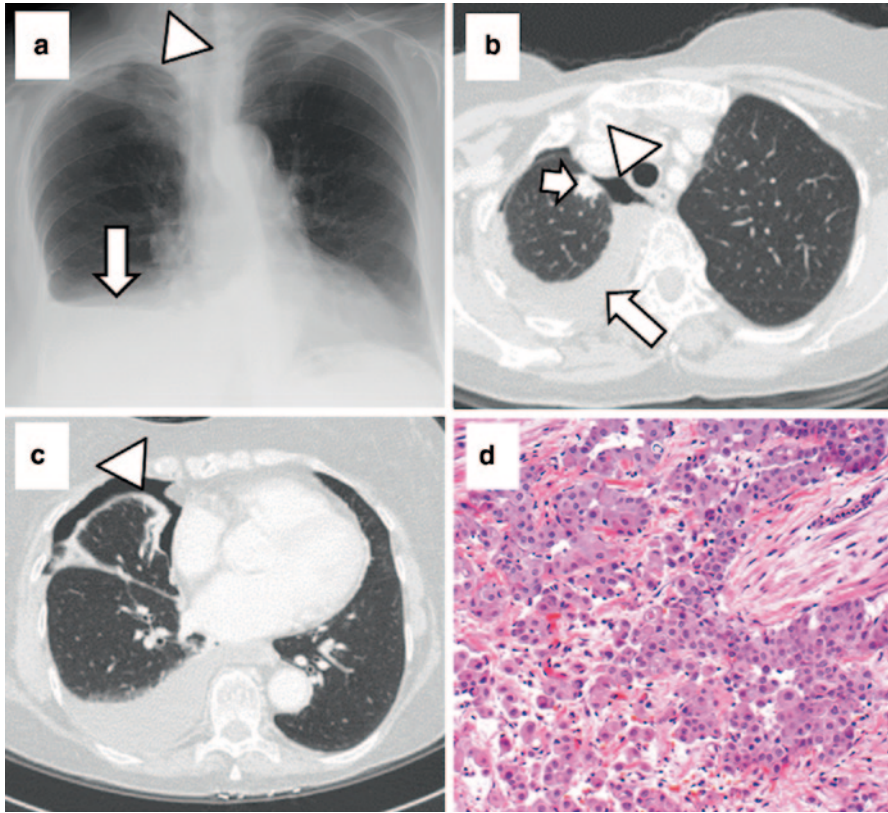
Fig. 3.1 This 80-year-old woman noted increasing exertional dyspnea over the past month along with dry cough. A chest X-ray revealed right-sided pleural fluid (*arrow*) and a small pneumothorax (*arrowhead*; hydropneumothorax) (**a**). A subsequent CT scan confirmed these findings (right-sided pleural effusion, *long arrow*; pneumothorax, *arrowhead*) and also revealed a 1.3 cm nodule in the right apex (*short arrow*), moderate volume loss of the right middle and lower lobes and thickening of the visceral pleura (**b**, **c**). The left lung and abdomen appear unremarkable. Biopsy from the right visceral pleura confirmed malignant mesothelioma, epithelioid type (**d**). *CT* computed tomography

Chest Pain

Chest pain in malignant pleural mesothelioma is most often of nonpleuritic quality, although pleuritic chest pain can also occur. In contrast to the nonpleuritic chest pain, pleuritic pain is typically characterized by a sudden, intense, and sometimes stabbing or shooting chest pain that is usually most severe when the lungs move during breathing, coughing, sneezing, or even talking. In a study by Adams et al., 62 patients (69 %) presented with chest pain; in 56 patients the chest pain was of nonpleuritic quality and only six patients had pleuritic chest pain [7].

Chest pain is generally caused by significant chest wall invasion by the malignant mesothelioma [2]. The pain might radiate to the upper abdomen, shoulder, or arm because of entrapment of intercostal thoracic, autonomic, or brachial plexus nerves. Involvement of the phrenic nerve by the mesothelioma might lead to hemidiaphragmatic paralysis. Occasionally, persistent chest wall pain precedes the development of either pleural masses or effusion by months and an initial chest X-ray might even be negative.

Less Common Signs and Symptoms

Cough may occur but is usually not a prominent symptom. Cough is more frequent in patients presenting with a pleural effusion [8].

The local expansion of the malignant mesothelioma sometimes leads to chest wall masses which, when invading into mediastinal structures, might impinge on large vessels, nerves, the esophagus, or the trachea or airways resulting in rare symptoms such as superior vena cava syndrome, hoarseness, Horner's syndrome, or dysphagia [3]. Invasion of the pericardium and the heart might lead to pericardial tamponade and arrhythmias.

Diffuse malignant pleural mesothelioma typically encases the lungs as a thick rind and grows along the fissures, while relatively sparing lung parenchyma; however, a few cases of malignant mesothelioma have been reported that clinically and radiologically mimic interstitial lung disease [9−13]. Larsen et al. described five cases of diffuse intrapulmonary malignant mesothelioma [9]. In those cases, the tumor had a preferential intraparenchymal growth pattern without significant pleural involvement. All five patients were men with a median age of 56 years. Patients presented with chronic dyspnea, cough, and acute dyspnea with bilateral pneumothorax, and were initially diagnosed as interstitial lung disease based on clinical and radiologic findings. Microscopic pleural involvement was identified in four cases. The median survival of three of the five patients treated with chemotherapy was 28 months [9]. Two patients received no therapy and survived 3 and 4 weeks, respectively.

Diffuse malignant pleural mesothelioma might spread to the abdomen and patients might present with ascites, constipation, or even bowel obstruction. Mesothelioma can also spread to the contralateral hemithorax resulting in bilateral pleural effusion [3].

In rare cases, malignant mesothelioma has been diagnosed at a prior incision site. Guenday et al. reported a 37-year-old woman who underwent pericardiocentesis for pericardial effusion with negative cytologic examination [14]. Seven months later, she presented with a skin lesion at the prior incision site which was found to be malignant mesothelioma. She was also diagnosed with pericardial malignant mesothelioma.

Lymphatic and hematogenous dissemination occurs late in the course of malignant pleural mesothelioma, and is identified fairly commonly in autopsy series. All organs can be involved. Metastatic disease has been described in liver, lung, heart, brain, meninges, thyroid, adrenal glands, kidneys, pancreas, bone, soft tissue, skin, and lymph nodes [15, 16]. Systemic lymphadenopathy is an exceedingly rare initial presentation of malignant mesothelioma with only a few cases being reported. In some of these case reports, the malignant mesothelioma was initially diagnosed in a lymph node, most commonly cervical, supraclavicular, or axillary, which initiated a search for the primary tumor, with peritoneal, pleural, or pericardial mesothelioma subsequently identified [17−21]. In one case of metastatic disease to the neck, the malignant pleural mesothelioma was not identified until 8 months after the initial diagnosis in the lymph node [22].

Other rare presentations include aphonia and dysphagia, abdominal distension, pressure sensation in the abdominal right upper quadrant, nausea, bad taste in the mouth, perceived tachycardia, headache, paraneoplastic syndrome, chest wall lump, lymphadenopathy, and hemoptysis [7, 23].

Time Interval Between Symptoms and Diagnosis

The average time interval between onset of symptoms and diagnosis is usually 2–3 months [3], but insidious and nonspecific symptoms may delay diagnosis up to 3–6 months or more [2, 24]. However, symptoms may present for an even longer time until a diagnosis is established, leading in some cases to long latency periods [5].

Location

Diffuse malignant pleural mesothelioma is slightly more common in the right pleura, and bilateral involvement at initial diagnosis is uncommon. A study by Adams found that the tumor was right sided in 55 % of patients, left sided in 41 %, and bilateral in 3 % [7]. Similarly, in the radiologic study by Seely, the right hemithorax was more commonly involved than the left (61 vs. 36 %, respectively), and 3 % of patients had bilateral involvement [6]. Tanrikulu et al. studied 363 patients with pleural mesothelioma and also showed that the majority of mesotheliomas were right sided (61 %), with only 7 % bilateral [24]. In a study of 272 patients with malignant mesothelioma in southeast England, right-sided disease were 1.6 times more common than left-sided disease based on clinical, radiologic, and autopsy data [25].

Table 3.2 Signs and symptoms of patients with diffuse malignant peritoneal mesothelioma

Signs and symptoms	Percent patients
Abdominal	
Abdominal distension/increasing abdominal girth [26, 30, 31]	30–80
Ascites [29, 31, 36]	36–90
Abdominal mass [31, 36]	11–30
Pain [30, 31, 36]	27–69
Hernia [30, 31]	7–12
Diarrhea [36]	17
Vomiting [36]	15
Nausea [31]	11
Bowel obstruction [31]	3
Systemic	
Fatigue [31, 36]	11–43
Weight loss [31, 36]	32–38
Anorexia [31, 36]	27–30
Fever [36]	22
No symptoms, incidental diagnosis [30, 35]	8–17

Diffuse Malignant Peritoneal Mesothelioma: Clinical Signs and Symptoms

There are no signs or symptoms that are specific for diffuse malignant peritoneal mesothelioma (Table 3.2). Due to the nonspecific nature of the presenting symptoms, many patients have already an advanced stage of the disease at the time of diagnosis. Radiological features of peritoneal malignant mesothelioma are also nonspecific and can include ascites and peritoneal thickening, nodularity, or masses with or without omental involvement. Differential considerations include peritoneal carcinomatosis, pseudomyxoma peritonei, peritonitis, cystic lymphangioma, and ovarian neoplasms.

Abdominal Distension

Abdominal distension and/or increasing abdominal girth is the most frequent initial symptom, occurring in 30–80 % of patients with peritoneal malignant mesothelioma [26−28]. It is usually due to ascites or may be due to tumor mass expansion within the abdominal cavity. Ascites is the most common sign, occurring in 90 % of the patients [29]. In contrast to patients with abdominal distension due to excess caloric intake or benign ascites associated with nonmalignant conditions (e.g., cirrhosis) where patients can gain weight, patients with mesothelioma often exhibit weight loss.

Pain

Pain is the second most common symptom in patients with diffuse malignant peritoneal mesothelioma, although in some studies, it was more common than abdominal distension [30, 31] (Fig. 3.2). In most cases, the pain is diffuse and nonspecific, although rarely, patients can present with an acute abdomen secondary to perforation or bowel obstruction [32].

Other Signs and Symptoms

Early satiety, dysphagia, and shortness of breath are other nonspecific symptoms that may occur in patients with peritoneal mesothelioma. These symptoms are likely due to ascites or an enlarging abdominal mass and they can contribute to weight loss, impaired performance status, and fatigue. Abdominal distension may manifest as a new or worsening abdominal wall hernia.

Gastrointestinal complications such as bowel obstruction are usually a manifestation of advanced disease and occur late in the course of the disease [26, 33]. A palpable abdominal mass, deep vein thrombosis, and arterial occlusion may also occur [26, 27].

Malignant peritoneal mesotheliomas of the abdominal cavity can occasionally clinically mimic ovarian tumors, especially in young women. Although malignant peritoneal mesothelioma can secondarily involve the ovaries, patients with malignant peritoneal mesothelioma characteristically present with abdominal disease rather than with ovarian masses. Mani et al. described seven cases of peritoneal mesothelioma in which the initial manifestation was an ovarian mass [34]. The patients, ranging from 22 to 52 years old, underwent surgery with a primary diagnosis of ovarian cancer, exhibiting masses measuring 3.8–9 cm. Four of the seven cases were predominantly cystic and three were solid tumors. Histologically, the cystic tumors were multicystic mesotheliomas, and the three solid tumors were diffuse malignant mesotheliomas.

Occasionally, malignant mesothelioma is an incidental finding during infertility surgery or other gynecologic surgery [30]. In a study of 75 women with malignant peritoneal mesothelioma, 13 (17%) were incidental surgical findings [35].

Time Interval Between Symptoms and Diagnosis

Similar to diffuse malignant pleural mesothelioma, the mean time interval between the onset of symptoms and the establishment of the diagnosis is typically 2–3 months. Manzini et al. found that the median diagnosis time (first symptoms to diagnosis) was 2 months (range, 0–29 months) [36]. Acherman et al. reported a mean
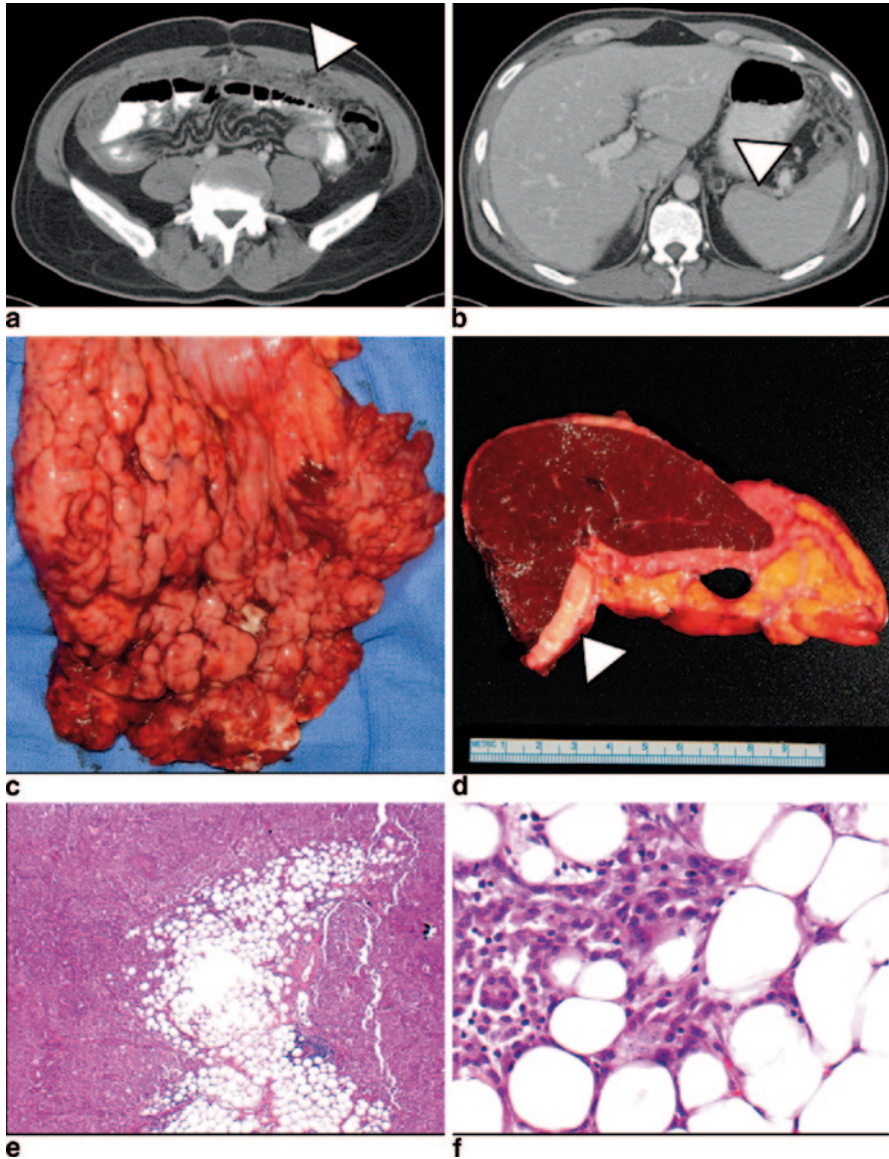
Fig. 3.2 This 48-year-old man presented with abdominal pain, some weight loss over several months, and fatigue. Work-up revealed anemia and a negative colonoscopy. His abdominal symptoms continued and about 2 weeks later, he presented to the emergency department. A CT scan of the abdomen showed diffuse thickening of the omentum (**a**, *arrowhead*) and peritoneal thickening surrounding the spleen (**b**, *arrowhead*). The chest appeared uninvolved. The patient underwent exploratory laparotomy. The omentum was diffusely involved by malignant mesothelioma forming a 38.0 cm mass (**c**) which was resected. The spleen was encased by malignant mesothelioma (**d**, *arrowhead*) and removed. An appendectomy and peritoneal stripping were also performed. Histologic examination, on low power view, shows sheets of epithelioid cells invading into adipose

diagnosis time of 10 months [30]. However, in a few patients, the time between symptoms and diagnosis has been reported in years, reflecting the lack of specific symptoms, the rarity of the disease, and the difficulty in distinguishing between diffuse malignant peritoneal mesothelioma and other primary or metastatic peritoneal tumors [26, 29]. In a study of 75 women with malignant peritoneal mesothelioma, Baker et al. identified four cases with delayed diagnosis between 2 months and 3 years [35]. In these four cases, a diagnosis of florid reactive or atypical mesothelial hyperplasia was made at initial surgery; however, later laparotomy for persistent symptoms showed malignant mesothelioma.

Clinical Presentations Common to Both Diffuse Pleural and Peritoneal Mesothelioma

Paraneoplastic Syndromes

Malignant mesothelioma can be associated with various paraneoplastic syndromes, including thrombocytosis [36], migratory thrombophlebitis, disseminated intra-vascular coagulation, venous thrombosis [37, 38], thrombotic thrombocytopenic purpura (TTP) [39], Coombs-positive hemolytic anemia, hypoglycemia [27], fever, paraneoplastic hepatopathy [27], sensory–motor polyneuropathy [40], Anti-Ma2 antibody-associated paraneoplastic syndrome (presenting with opsoclonus and diffuse cerebellar signs) [41], anti-Yo-related paraneoplastic cerebellar degeneration [42], renal disease, and hypercalcemia. These paraneoplastic syndromes are of course not unique to malignant mesothelioma and also have been described in other malignancies. Paraneoplastic syndromes are generally seen in the context of advanced disease; however, in some cases, malignant mesothelioma is diagnosed during the workup of the paraneoplastic syndrome. Archer et al. reported a sarcomatoid mesothelioma patient with opsoclonus and diffuse cerebellar signs who had an anti-Ma2 antibody-associated paraneoplastic syndrome [41]. Socola et al. reported a patient who presented with recurrent, rapidly relapsing episodes of thrombotic thrombocytopenic purpura associated with severe abdominal pain culminating in an acute abdomen who was found to have diffuse malignant peritoneal mesothelioma with tumor located in the left side of the pelvis encasing the distal sigmoid colon [39]. Banayan et al. reported a case of a 45-year-old woman with recurrent

tissue (**e**). High power view confirms large atypical epithelioid cells with prominent nucleoli. Immunostains performed on a previous biopsy showed that the neoplastic cells are positive for CK7, calretinin, CK5/6, and WT-1, and negative for CK20, synaptophysin, and chromogranin (not shown). The morphologic and immunophenotypic features are consistent with malignant mesothelioma, epithelioid type (**f**), (Magnification ×40[e], ×400[f]). The patient was treated with chemotherapy to which he appeared to have responded but subsequently developed ascites and recurrent disease and died 1.5 years later. *CT* computed tomography. (C&D: Courtesy of Dr. Florencia G. Que, Mayo Clinic Rochester, MN)

jugular vein thrombosis associated with weight loss, weakness, and anemia; who on workup was found to have peritoneal mesothelioma [38].

Some patients develop a paraneoplastic syndrome after mesothelioma diagnosis. Tanriverdi et al. reported a 51-year-old woman who was diagnosed with malignant pleural mesothelioma and underwent chemotherapy [42]. Two weeks after completion of the chemotherapy, the patient developed anti-Yo-related paraneoplastic cerebellar degeneration. Bech and Sorensen described a 57-year-old man with malignant pleural mesothelioma who developed sensory–motor polyneuropathy 18 days after diagnosis of the mesothelioma [40]. Extensive workup could not identify a specific cause for those symptoms and therefore a paraneoplastic syndrome was suspected. The patient was treated with immunoglobulin and prednisolone with improvement of the symptoms.

Constitutional Symptoms

Malignant mesothelioma patients might present with constitutional symptoms such as fatigue, hyperhidrosis, weight loss, tiredness, or sweating. They may also exhibit dry cough, fever, or night sweats [2]. These symptoms are usually found at advanced stage of the disease. In a study of malignant peritoneal mesotheliomas, vomiting was associated with worse survival [36].

Demographics of Malignant Mesothelioma

Because malignant mesothelioma most commonly is associated with occupational asbestos exposure, the disease is more common in men than in women and more frequent in advanced ages [2]. Therefore, diffuse malignant mesothelioma is usually a disease of adult men.

Overall, malignant pleural mesotheliomas are more common than malignant peritoneal mesotheliomas. Epidemiological studies have shown that peritoneal tumors once comprised approximately 30 % of all malignant mesotheliomas [42]; in some case studies, peritoneal mesotheliomas outnumbered pleural mesothelioma. For instance, Ribak et al. [30] studied 2271 consecutive deaths among 17,800 asbestos insulation workers in the USA and Canada (1967–1984); 134 patients had pleural and 222 had peritoneal mesotheliomas. Furthermore, of 86 Swedish insulation workers who died between 1970 and 1994, seven died of malignant peritoneal mesothelioma but none of pleural mesothelioma [43]. However, the percentage of peritoneal mesotheliomas dropped to approximately 7–17 % of all mesotheliomas in more recent years [42, 44−46]. This probably is not due to a decreasing incidence of peritoneal mesotheliomas, but rather an increased occurrence of pleural mesothelioma possibly due to an increased intensity of exposure [42].

Because of the relative rarity of pleural mesotheliomas in women, the ratio of peritoneal to pleural mesotheliomas is higher in women (1:2) than in men (1:5) [34].

Malignant Pleural Mesothelioma

Men comprise 60–84 % of all cases of malignant pleural mesothelioma [6, 7, 23, 24]. The mean age for men with malignant pleural mesothelioma has been reported between 54 and 59 years with an age range from 20 to 77 years [7, 23]. The mean age for women is very similar and described between 55 and 60 years, ranging from 24 to 80 years [7, 23]. In studies that did not report age by gender, the mean age for malignant pleural mesothelioma was between 51 and 68 years with reported age ranges from 19 to 88 years [6, 24, 30]. However, although rare, malignant pleural mesotheliomas have also been described in children [47, 48].

Malignant Peritoneal Mesothelioma

Similar to diffuse malignant pleural mesotheliomas, peritoneal mesotheliomas are more commonly reported in men than women. In a study of 81 patients with malignant peritoneal mesotheliomas, 57 men (70.4 %) and 24 women were included [35]. Acherman et al. [29] reported that out of 51 patients with malignant peritoneal mesothelioma, 34 were men (66.7 %).

In a study of 75 malignant peritoneal mesotheliomas in women, the mean age was 47.4 years with an age range from 17 to 92 years [34]. In other studies, the mean age for men was between 51.2 and 63.0 years and for women between 48.7 and 68.0 years [29, 35].

Malignant peritoneal mesotheliomas have rarely been described in children [48, 49].

Laboratory Findings

Pleural Effusion

Effusions in malignant mesothelioma are of exudative quality as established by Light criteria [50] that include one or more of the following: (1) pleural fluid/serum (PF/S) protein ratio greater than 0.5; (2) PF/S lactate dehydrogenase (LDH) greater than 0.6; and (3) pleural fluid LDH level greater than two-thirds of the serum upper limit of normal [51]. Gottherer et al. characterized the pleural fluids of 26 patients with diffuse malignant pleural mesothelioma [52]. (Table 3.3). All pleural fluids

Table 3.3 Characteristics of pleural fluid in malignant pleural mesothelioma based on findings by Gottehrer et al. [52]

Pleural fluid analyte	Mean (range)
Glucose (mg/dL)	75 (13–222)
Glucose PF/S	0.64 (0.1–1.07)
LDH (IU/L)	516 (53–2,364)
LDH PF/S	3.21 (0.55–21.3)
Protein (g/dL)	4.3 (1.9–5.7)
Protein PF/S	0.64 (0.27–0.85)
WBC (per microL)	1,617 (55–10,800)
RBC (per microL)	56,363 (19–560,000)

PF/S pleural fluid/serum ratio, *WBC* white blood cell count, *RBC* red blood cell count

were determined to be exudative by protein and LDH levels. The pleural fluid of nine (of 17) patients had a low pH (<7.30, range 6.92–7.26); in eight patients, the pleural fluid had a pH of ≥ 7.30. The study showed that patients with lower pleural fluid pH and PF/S glucose ratio had a shorter survival. In a study by Tanrikulu et al., a pleural fluid glucose level of ≤ 40 mg/dL and a serum LDH level of ≤ 500 U/L was associated with poor survival [24].

Biomarkers for Malignant Mesothelioma

Research has focused on the identification of serological and fluid markers for diagnosis, response to treatment, and prognosis of malignant mesothelioma. Although some promising candidate markers have been studied, currently, there are no serologic or fluid markers to aid in establishing a diagnosis of malignant mesothelioma because low sensitivity and specificity do not allow for their use in routine clinical practice. However, evidence suggests that some markers might be useful in the follow up of patients after treatment to identify possible recurrence and/or progression of disease. Other markers might have some prognostic value. Some of the more recently studied biomarkers include fibulin-3, mesothelin, and osteopontin.

Fibulin-3 is an extracellular glycoprotein that is encoded by the *epidermal growth factor-containing fibulin-like extracellular matrix protein (EFEMP1)* gene. Recently, Pass et al. showed that plasma and effusion fibulin-3 levels were significantly higher in patients with pleural mesothelioma than in asbestos-exposed people without mesothelioma [53]. These studies concluded that in conjunction with effusion fibulin-3 levels, plasma fibulin-3 levels might be able to differentiate mesothelioma effusions from other malignant and benign effusions. However, additional studies will be required to determine the role of fibulin-3 as a biomarker for diagnosis and monitoring patients after initial treatment.

Mesothelin, a glycoprotein that is expressed on the surface of benign mesothelial cells, was found to be overexpressed in some malignant mesothelioma. Soluble mesothelin-related peptides (SMRPs) are thought to be a splice-variant of mesothelin that can be found in serum and pleural fluid [54]. Elevated levels of SMRP have been identified in epithelioid but not sarcomatoid mesotheliomas. However, mesothelin can also be increased in other tumors such as ovarian carcinoma, pancreatic carcinoma, and lung cancers or in renal insufficiency. Furthermore, the sensitivity and specificity appear to depend on the detection method and cutoff values used and therefore, further studies are necessary to establish the diagnostic and prognostic importance of that biomarker.

Osteopontin is a glycoprotein that mediates cell–matrix interactions and is overexpressed in several types of cancers. Pass et al. showed that serum osteopontin levels were significantly higher in patients with malignant pleural mesothelioma than in patients with exposure to asbestos [55]. Furthermore, tumor cells stained for osteopontin in 36 of 38 cases of pleural mesothelioma. However, further studies are necessary to confirm those data.

Carcinoembryonic antigen (CEA) has also been studied for its use in malignant mesothelioma. A meta-analysis of 11 studies that identified the value of CEA to distinguish between malignant mesothelioma and metastatic lung cancer showed that the sensitivity of CEA for malignant pleural mesothelioma ranged from 0.73 to 1.00 (mean 0.97, 95 % CI: 0.93–0.99) when the CEA assay was negative [56]. Interestingly, in 8 of 11 studies the sensitivities were 1.00 and only one study showed a relative low sensitivity (0.73). Therefore, a high pleural fluid CEA might assist in ruling out malignant mesothelioma, and the pleural fluid CEA assay might be useful in helping distinguish malignant pleural mesothelioma from metastatic lung cancer.

Hyaluronic acid (HA) has been proposed as a putative diagnostic marker because its level is increased in approximately 60 % of pleural effusions from patients with malignant mesothelioma [57]. On the other hand, Fuhrman et al. did not show a significant difference in HA of pleural fluid between benign pleural effusion and effusion associated with malignant pleural mesothelioma; however, HA was significantly higher in mesothelioma than in nonmesothelioma malignancies [58]. In the serum, elevated HA levels have been described only in advanced stage mesothelioma [59]; and a significant percentage of malignant mesothelioma may not secrete HA [58, 60].

Studies suggest that a combination of biomarkers might be superior to the use of any single marker. Creaney et al. showed that a combination of effusion HA, and serum and effusion mesothelin had a greater diagnostic accuracy than effusion mesothelin alone [61]. Furthermore, SMRP might improve CYFRA-21–1 and CEA accuracy in pleural effusion in the differential diagnosis of malignant pleural mesothelioma [62]. Further studies are necessary to identify a combination of biomarkers that might be helpful in the diagnosis, prognosis, and disease progression of malignant mesothelioma.
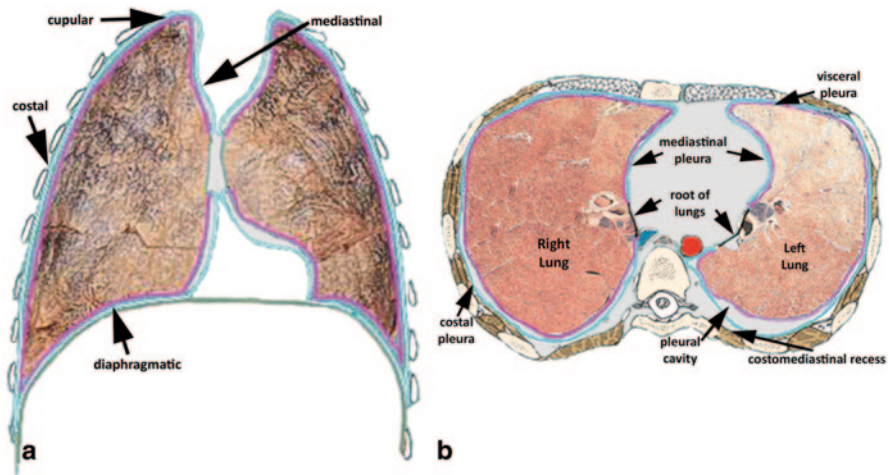
Fig. 3.3 Schematic images illustrate the gross anatomic locations of pleural anatomy (**a**) and the relationships of the parietal (*blue*) and visceral *(purple)* pleura to each other. The anteroposterior relationship of this anatomy is shown in (**b**) and correlates with what is seen on conventional axial CT image acquisitions. *CT* computed tomography. (Reprinted with permission of Dr. Wesley Norman, "The Anatomy Lesson," 1999)

Clinical and Radiological Staging of Malignant Pleural Mesothelioma

Staging of malignant pleural mesothelioma sets the stage for therapeutic management and overall outcome. Radiologic staging, as such, involves a pattern search that is based largely on pleural anatomy which is not necessarily straightforward. Pleural anatomy is grossly partitioned into the cupola or cervical pleura, the mediastinal pleura, the costal pleura, and the diaphragmatic pleura [63, 64]. The cervical pleura surrounds the apices of the lungs and can extend into the neck as much as 5 cm above the sternal end of the first rib. The mediastinal pleura adheres to the pericardium with phrenic nerve coursing between them. The costal pleura lies immediately adjacent to loose connective tissue called the endothoracic fascia which abuts the thoracic wall (the sternum, costal cartilages, ribs, and chest wall muscles), and the diaphragmatic pleura covers the diaphragm except for the central tendon. The inferior aspect of the pleura extends to the T12 vertebral body with the approximate inferior extent of the pleura being about two fingerbreadths inferior to the lung. Posteriorly, the pleura is reflected upon the side of the vertebral bodies. (Fig. 3.3a, b)

Knowledge of pleural lymphatic drainage is helpful in radiological staging. Lymphatic drainage of the visceral pleura and the lung are the same; however, lymphatic drainage of the parietal pleura can be complex. The anterior parietal pleura drains into the internal mammary lymph nodes. The posterior parietal pleura drains into paraspinal lymph nodes. Anteriorly, the diaphragmatic pleura drains into internal

mammary and anterior diaphragmatic lymph nodes while posteriorly, it drains into para-aortic and posterior mediastinal lymph nodes. In the setting of suspected malignant pleural mesothelioma, any lymph nodes in the extrapleural space are best viewed with suspicion.

The present TNM (tumor, node, metastasis) system (Table 3.4) is based on the largest, multicenter and international database on malignant pleural mesothelioma from the International Association for the Study of Lung Cancer (IASLC), and is able to classify patients into different outcomes [65−67]. Using the TNM descriptors, staging of malignant pleural mesothelioma has been established (Table 3.5) [65].

Analysis of the IASLC database has shown that the survival of malignant pleural mesothelioma is significantly affected by the overall tumor stage ($p<0.0001$), T classification ($p<0.0001$), N classification ($p<0.0001$), tumor histology ($p<0.0001$), patient gender ($p=0.0002$) and age ($p=0.0025$), and type of operation (curative versus palliative, $p<0.0001$) [66]. Also shown in that analysis were statistically significant differences in survival between adjacent paired stages (except stage I vs. II), adjacent paired T categories (except T1 vs. T2), and adjacent paired N categories (except N1 vs. N2). Currently, clinical outcome depends a great deal on the ability of imaging to distinguish between stages II and III, III and IV, or between T2 and T3, or T3 and T4 disease, or between N0 and N1, or N2 and N3 disease. Distinction between potentially resectable (T3) and unresectable (T4) disease remains challenging, and unfortunately, as detailed below, limitations of imaging have not precluded the need for surgical staging to make this decision.

Radiologic Features

The primary role of imaging in malignant mesotheliomas lies in preoperative staging and assessment of treatment response, disease recurrence, or metastasis. Initial screening of the chest, regardless of clinical suspicion, often begins with a chest radiograph, largely due to accessibility and lower cost. Chest radiographs, depending on the number of views, generally cost around US$ 150–200. Additional characterization with cross-sectional imaging techniques, more often with CT than with magnetic resonance imaging (MRI) or positron emission tomography/computer tomography (PET/CT) are also performed with varying degrees of sensitivity and specificity. At present, a CT costs roughly US$ 1500; and, MRI and PET/CT are more expensive with an MRI costing about twice that of a CT and a PET/CT about twice that of an MRI. Of the cross-sectional imaging modalities, CT is most frequently obtained, again largely because of accessibility and cost when compared to PET/CT and MRI. Ultrasonography, another cross-sectional imaging technique, has been used but it is generally performed for targeted evaluation given the superior coverage afforded by the other imaging modalities. Endobronchial ultrasound or EBUS is performed by interventional pulmonologists and is not included in this section.

Table 3.4 The international association for the study of lung cancer (IASLC) malignant pleural mesothelioma staging system

| T—Primary tumor	
T1	
T1a	Tumor limited to ipsilateral parietal pleura, including mediastinal and diaphragmatic pleura; no involvement of the visceral pleura
T1b	Tumor involving the ipsilateral parietal pleura including mediastinal and diaphragmatic pleura; scattered foci of tumor also involving visceral pleura
T2	
	Tumor involving each of the ipsilateral pleural surfaces (visceral, parietal, mediastinal, and diaphragmatic) with at least one of the following features:
	Involvement of diaphragmatic muscle
	Confluent visceral pleural tumor (including fissures), or extension of tumor from visceral pleura into underlying pulmonary parenchyma
T3 Locally advanced but potentially resectable tumor	
	Tumor involving all of the ipsilateral pleural surfaces (visceral, parietal, mediastinal and diaphragmatic) with at least one of the following features:
	Involvement of endothoracic fascia
	Extension into mediastinal fat
	Solitary, completely resectable focus of tumor extending into the soft tissues of the chest wall
	Non-transmural involvement of the pericardium
T4 Locally advanced technically unresectable tumor	
	Tumor involving all of the ipsilateral pleural surfaces (visceral, parietal, mediastinal and diaphragmatic) with at least one of the following:

Table 3.4 (continued)

T—Primary tumor	
	Diffuse extension or multifocal masses of tumor in the chest wall, with or without associated rib destruction
	Direct transdiaphragmatic extension of tumor to the peritoneum
	Direct extension of tumor to the contralateral pleura
	Direct extension of tumor to one or more mediastinal organs
	Direct extension of tumor into the spine
	Tumor extending through the pericardium to internal surface of pericardium with or without pericardial effusion; or tumor involving the myocardium
N—Lymph nodes	
NX	Regional lymph nodes cannot be assessed
N0	No regional lymph node metastases
N1	Metastases in ipsilateral bronchopulmonary or hilar lymph nodes
N2	Metastases in subcarinal or ipsilateral mediastinal lymph nodes, including ipsilateral internal mammary nodes
N3	Metastases in contralateral mediastinal, contralateral internal mammary, ipsilateral or contralateral supraclavicular lymph nodes
M—Metastases	
MX	Distant metastases cannot be assessed
M0	No distant metastases
M1	Distant metastases present

**Table 3.5** Clinical and TNM staging of malignant pleural mesothelioma

Stage	Tumor	Node	Metastasis
Ia	T1a	N0	M0
Ib	T1b	N0	M0
II	T2	N0	M0
III	Any T3	Any N1 or N2	M0
IV	Any T4	Any N3	Any M1

Chest Radiographs

Conventional chest radiograph provides two views of the chest, a posterior–anterior (PA) view and a lateral view. In the absence of pleural disease, the pleura is generally appreciated simply as the "edge" of the relatively radiolucent lungs. Pleural disease usually manifests as circumferential pleural thickening that often has better conspicuity where the X-ray beams are perpendicular to the pleura—laterally and medially on the PA view and anteriorly and posterior on the lateral view. Radiographic appearances of pleural disease are quite variable and can include a normal appearance particularly in early disease, pleural thickening (focal, diffuse, or nodular), pleural effusion, pleural mass, or complete hemithorax opacification (Fig. 3.4). When the pleura is diffusely thickened, a rind of soft tissue often has a nodular or scalloped appearance that becomes more obvious with more advanced disease (Fig. 3.5). A single anterior–posterior (AP) chest radiograph is generally performed on hospitalized patients who are unable to
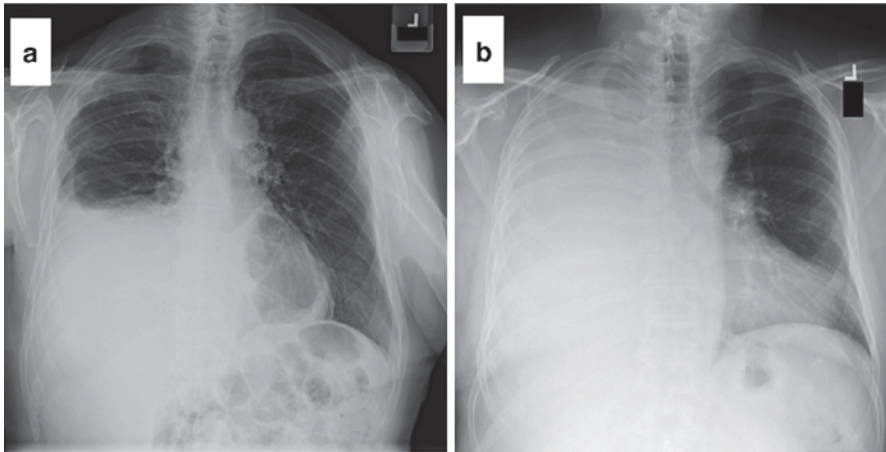
Fig. 3.4 Two different patients with malignant pleural mesothelioma illustrating unilateral right-sided pleural effusion. In **a**, there is a moderate to large pleural effusion and pleural thickening. In **b**, opacification of the right hemithorax is not associated with significant mediastinal shift; in particular, there is no significant mediastinal shift toward the opacification. Differential considerations include mass (pleural, chest wall, or pulmonary), pleural effusion, and consolidation
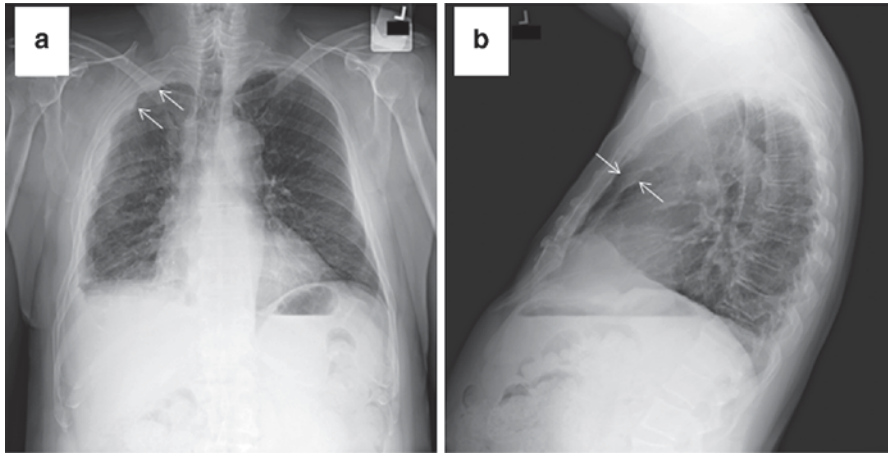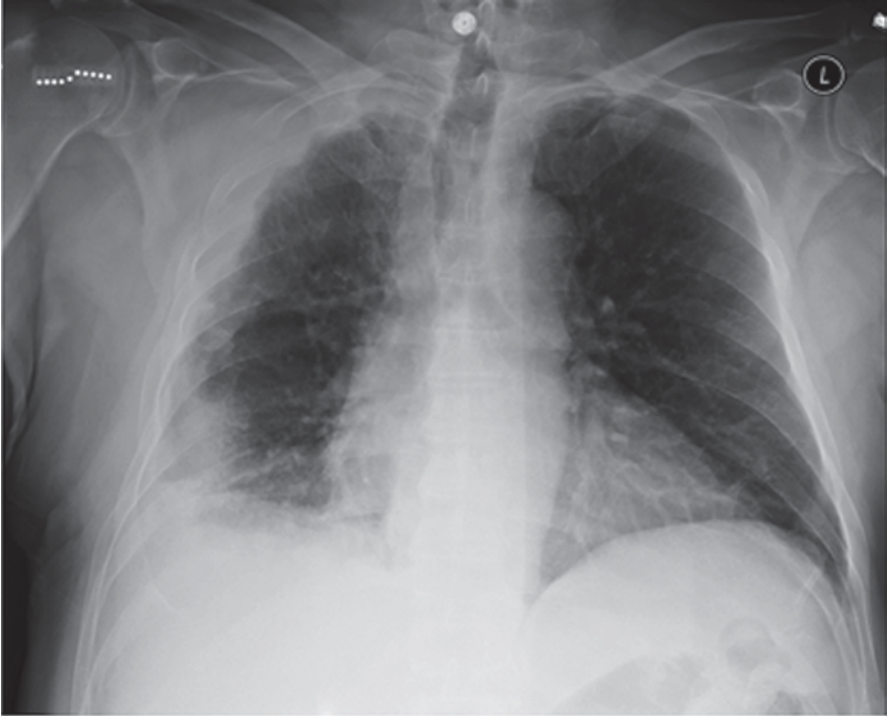
Fig. 3.5 Posterior–anterior (**a**) and lateral (**b**) chest radiographs of the same patient with malignant pleural mesothelioma. Note the nodular pleural thickening that partially encases the right lung (*arrows*) which has relative decreased lung volume compared to the left lung. On the lateral view (**b**), the nodular pleural thickening is best appreciated anteriorly (*arrows*). Notice also the lucent left costophrenic angle but blunted right costophrenic angle which could be from pleural thickening or fluid

assume an upright position (Fig. 3.6). How much the patient is "propped up" is generally indicated on the film. The radiographic signs that suggest early disease include asymmetric volume loss of the involved lung over the contralateral one (in the setting of unilateral disease; Fig. 3.7), and unilateral pleural effusion.

Computed Tomography

CT is the primary workhorse in imaging evaluation of malignant mesothelioma. Many of the CT features described for malignant mesothelioma over a decade ago [68] still apply today. There remains great variability in the pleural CT imaging features of malignant pleural mesothelioma, ranging from nonspecific plaques (noncalcified and calcified) to focal masses to diffuse irregular or nodular pleural thickening encasing the entire lung. (Fig. 3.8) With CT, more detailed assessment of the chest wall, pericardium, mediastinum, diaphragm, and major vessels can be made. In a study of 215 patients with pleural disease, 99 of which with malignant pleural mesothelioma, multivariate analysis resulted in three CT findings for differentiating mesothelioma from metastatic pleural disease; these included (i) rind-like pleural involvement (sensitivity/specificity 70/85 %), (ii) mediastinal pleural involvement (sensitivity/specificity 85/67 %), and (iii) pleural thickness more than 1 cm (sensitivity/specificity 59/82 %) [69]. Evidence of unilateral volume loss can be supported by elevation of the ipsilateral hemidiaphragm, ipsilateral shift of the mediastinum, and narrowing of the intercostal spaces.

Fig. 3.6 Anterior–posterior chest radiograph of the same patient as in Fig. 3.4, who was later hospitalized. Note the indicator for the degree of inclination projected over the upper right humeral head. Notice nodular pleural thickening on the right and the relatively smaller right lung compared to the left
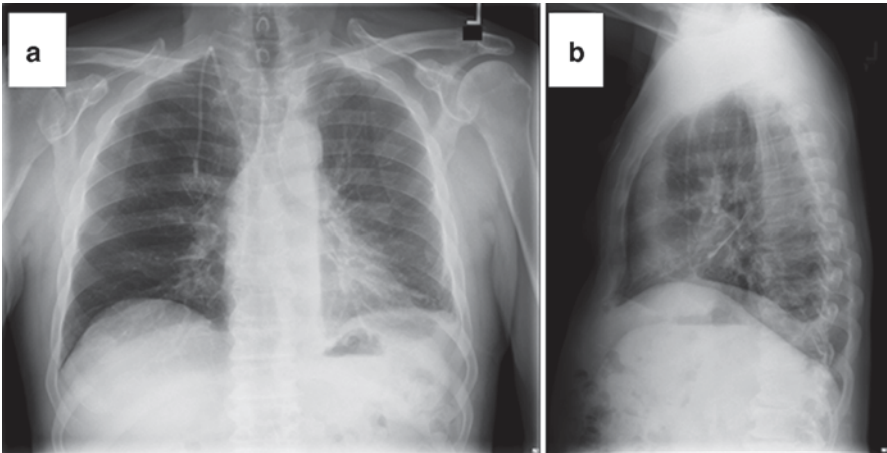

Fig. 3.7 Chest radiograph—posterior–anterior (**a**) and lateral (**b**)—shows a small left pleural effusion and decreased left lung volume compared to the right. There is also left pleural thickening
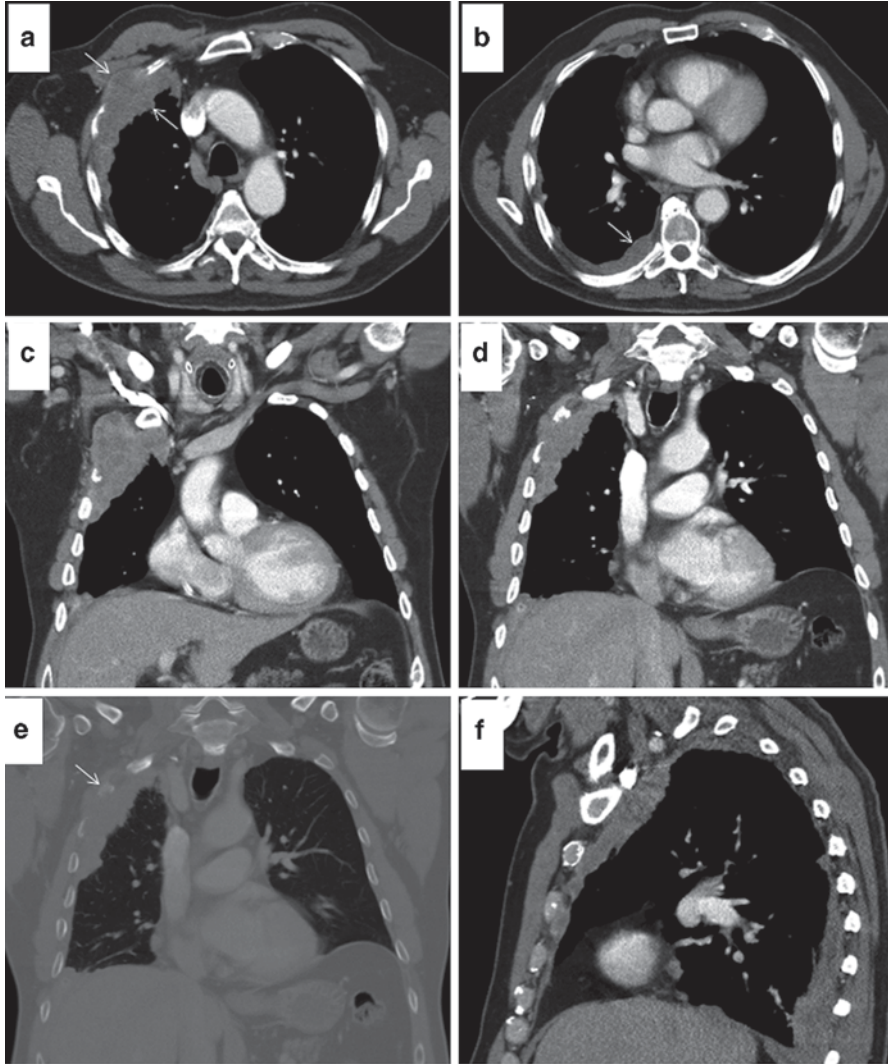
Fig. 3.8 Contrast-enhanced chest CT axial images (**a**, **b**) of a patient with malignant meso-thelioma demonstrate nodular pleural thickening on the right (*arrows*). Coronal reformatted views (**c**, **d**) show extension of the anterolateral component of the pleural thickening into the chest wall with destruction of the overlying ribs which are confirmed on bone windows (*arrow*) (**e**). A sagittal reformatted view (**f**) offers another opportunity to assess for the extent of disease. *CT* computed tomography

CT can be performed with or without intravenous iodinated contrast. Often, in-travenous contrast is administered in the setting of malignant mesothelioma because the additional soft tissue contrast and enhanced conspicuity of details generally can help the radiologist assess for effacement of fatty planes by infiltrative disease at the mediastinal (particularly pericardial), diaphragmatic, pleural, and chest wall levels.
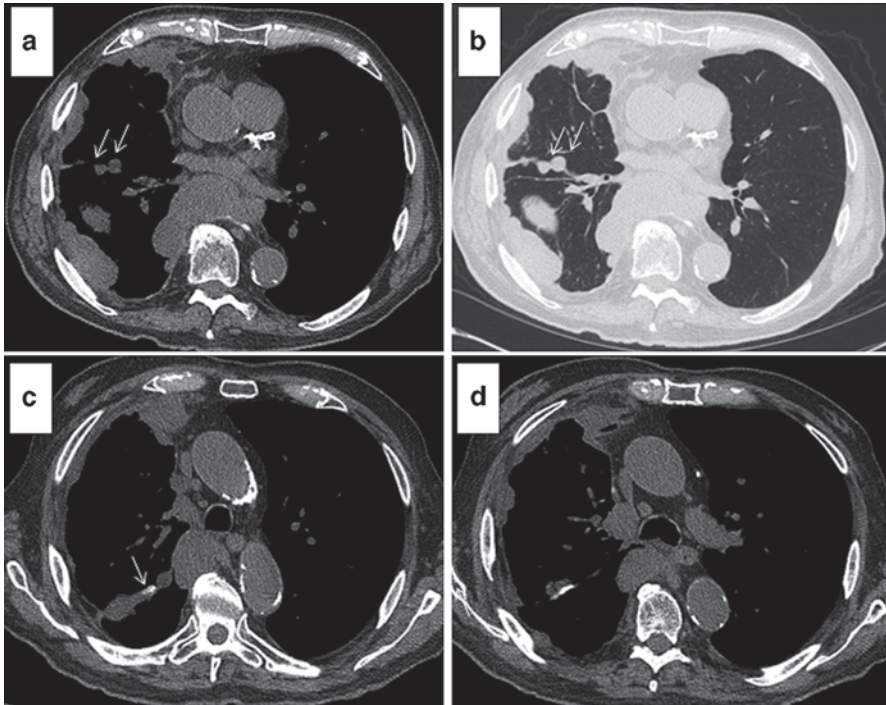
Fig. 3.9 A single axial slice of a noncontrast enhanced CT **a** of a patient with malignant pleural mesothelioma, including corresponding lung windows **b** demonstrates nodular pleural thickening on the right side that extends into the right major fissure (*arrows*). The right lung volume is smaller than the left. Two other axial slices **c**, **d** show nodular pleural thickening with associated calcifications (*arrow*), also extending into the right major fissure. *CT* computed tomography

Another use of intravenous contrast, particularly as a way to assess hemodynamic function or perfusion of disease, is still at an investigatory stage [70].

Determination of parietal involvement by disease is important in staging. Despite the very high in-plane resolution of CT, the distinction between normal visceral and parietal pleura is extremely challenging; the distinction is much easier in the setting of pleural effusion and sometimes in the setting of pleural masses. An investigation into using Hounsfield units, which indicate CT attenuation or radiodensity of the image pixels, has shown that malignant pleural mesothelioma soft tissue tends to have Hounsfield units that fall between pleural effusion and muscle and liver [71]. This overlap makes it challenging for imaging to adequately distinguish the extent of disease, particularly across tissue planes. Without intravenous contrast and even in some cases with intravenous contrast, the soft tissue contrast differences between pleura, endothoracic fascia, and even chest wall can be nearly impossible to ascertain with certainty. Involvement of the interlobar fissural pleura is characteristic of mesothelioma (Fig. 3.9) and can be sometimes more apparent on reformatted sagittal or coronal views compared to the conventional axial views.

CT staging of malignant pleural mesothelioma for extrapleural involvement includes the chest wall with particular attention to the ribs and spine, the mediasti-

num with particular attention to the pericardium and extension into the contralateral hemithorax, lymph node involvement including the hilar, middle mediastinal, internal mammary, anterior diaphragmatic regions, as well as hemidiaphragmatic involvement with particular attention to transdiaphragmatic involvement. The literature has shown high sensitivity (>90%) of both CT and MRI in the ability to assess for resectability especially for evaluation of the chest wall, mediastinum, and diaphragm [72] but the specificity of these imaging studies is more disappointing. Detection of diaphragmatic invasion is still challenging by CT, and while MRI can provide additional information, surgical staging in this region is often warranted.

Magnetic Resonance Imaging

MRI uses a nonionizing technique for image acquisition, and patients loosely know it as the "no radiation" scan. MRI provides exquisite soft tissue detail and contrast, and the physical phenomenon measured with the MRI technique can give some insight into the nature of the soft tissue make-up of its components. Multiplanar acquisitions widen imaging approaches and cardiac gated and respiratory compensation techniques reduce much of the motion artifacts which used to preclude diagnostic use of MRI in the chest. In a prospective study, CT and MRI were nearly equivalent in diagnostic accuracy of staging; however, MRI was superior to CT in revealing diaphragmatic invasion, endothoracic fascia invasion, and in showing solitary resectable foci of chest wall invasion [73]. The different T1 and T2 relaxivities of soft tissues are accentuated on T1-weighted and T2-weighted non-contrast-enhanced techniques. Malignant pleural mesothelioma tends to have slightly higher T2 signal which is accentuated with fat suppression (Fig. 3.10). With intravenous gadolinium-based contrast agents, some of the soft tissue detail is accentuated (Fig. 3.11).

Diffusion-weighted imaging (DWI) is an MRI technique that reflects the degree of Brownian motion of the protons (essentially from water molecules) within soft tissue. As such, water protons whose diffusivity is restricted by increased cellularity (such as in malignancies) or by debris or macromolecules (such as in abscesses) will be higher signaling on diffusion-weighted imaging (Fig. 3.12). The restricted diffusivity of these protons is reflected in a quantitative metric called the apparent diffusion coefficient (ADC). Initial experience with DWI at 3T has shown promise for differentiating malignant pleural disease from benign disease with improvement of sensitivity with dynamic contrast-enhanced MRI [74]. The "pointillism sign" described as hypersignaling foci on DWI obtained at high diffusion sensitivities or b-values (Fig. 3.13) is thought to be caused by multifocal deposits of tumor [74]. This suggests that this might be a way for targeted biopsy, but ongoing investigation continues in this area.

Imaging assessment for disease progression or treatment response is challenging in malignant pleural mesothelioma. A modified response evaluation criteria in solid tumor (RECIST) approach for measuring such disease [75] is available given interobserver and intraobserver variability and is often used in clinical trials and staging protocols as well as in evaluating treatment response. Investigations continue on volume measurements of disease from imaging [76]. Fast image acquisi-
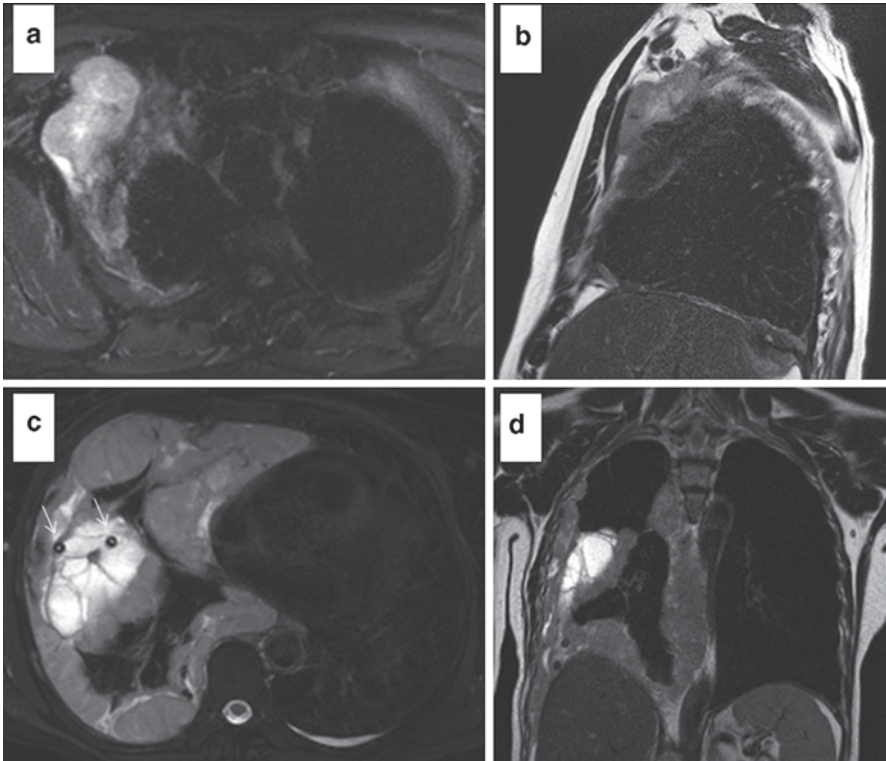
Fig. 3.10 Multiplanar T2-weighted MRI acquisitions of two patients with malignant pleural mesothelioma. Axial fat-suppressed T2-weighted image **a** of one patient demonstrates pleural nodularity on the right side that extends into the chest wall where it appears as a lobulated mass with some central necrosis. Sagittal nonfat suppressed T2-weighted image acquisition **b** of the same patient shows soft tissue signaling distinction between the chest wall mass, the overlying muscles, and the adjacent fat. In a different patient with malignant pleural mesothelioma, axial fat-suppressed T2-weighted image **c** demonstrates a thickened nodular pleural "rind" on the right side, loculated, complex, septated pleural fluid, and two round susceptibility artifacts (*arrows*) consistent with parts of a chest tube. A coronal non-fat-suppressed T2 weighted image (**d**) shows soft tissue contrasts between the thickened pleura and the hemidiaphragm. *MRI* magnetic resonance imaging

tion techniques, such as steady state free precession sequences, are fast enough to acquire images while the patient is breathing. Images acquired in this manner allow for evaluation of hemidiaphragmatic motion which can be limited by diaphragmatic tumor invasion or by disease invading the phrenic nerve.

Positron Emission Tomography/Computer Tomography

With its ability to provide information on tumoral metabolic activity as well as anatomic information, PET/CT has been useful in distinguishing benign from malig-
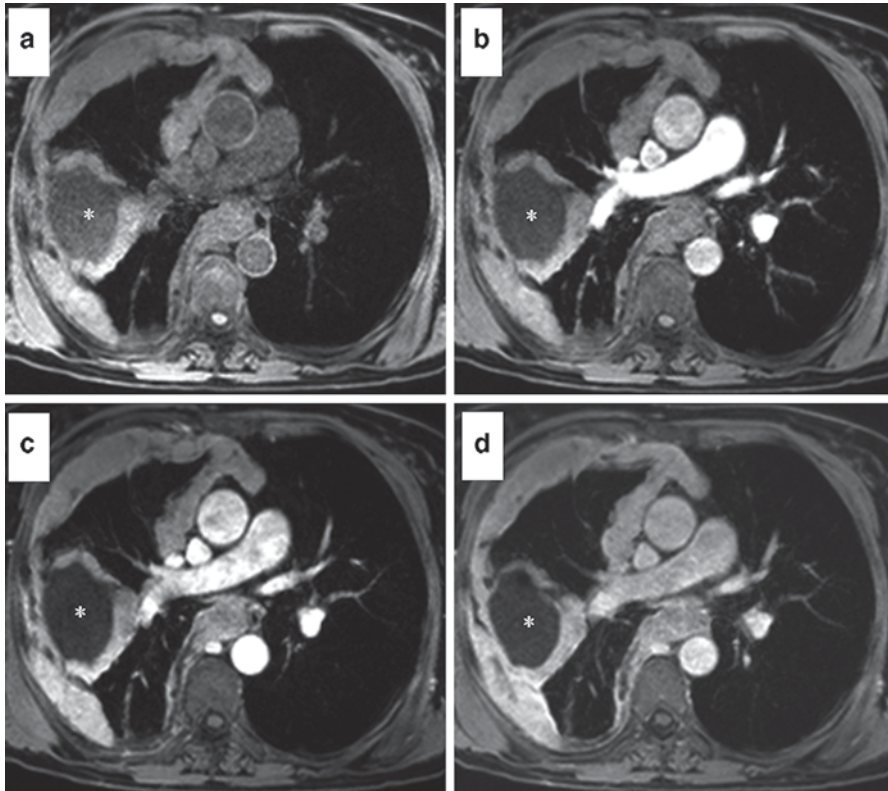
Fig. 3.11 Axial MRI acquisition before intravenous contrast administration (**a**) and three image acquisitions obtained at three different time points after contrast administration (**b–d**; i.e., dynamic contrast-enhanced MRI) demonstrate mostly persistent enhancement of the thickened pleura on the right. The loculated pleural effusion (*) which was seen on Fig. 3.9c shows no enhancement. *MRI* magnetic resonance imaging

nant pleural disease and in the staging, post-therapeutic follow-up, and prognosis of malignant pleural mesothelioma [70, 77−79] (Fig. 3.14). In 63 consecutive patients with histologically proven malignant pleural disease, the sensitivity of PET/CT for detecting malignancy was 96.8% with a negative predictive value of 93.9%, while its specificity was 88.5% and its positive predictive value was 93.8% [80]. Various investigations have shown that its primary advantage is one of identifying distant metastases. Standardized uptake values or SUVs are metrics that provide the relative tissue/organ uptake. Despite a relatively large degree of variability of SUVs due to biological, physical, processing, and acquisition errors, SUVs as a form of molecular imaging can facilitate therapy monitoring as well as management decisions [81, 82]. PET/CT plays are large role in the imaging evaluation of malignant pleural mesothelioma, but it, too, is limited in its ability to specify disease infiltrating across tissue planes, often requiring surgical staging or assessment.
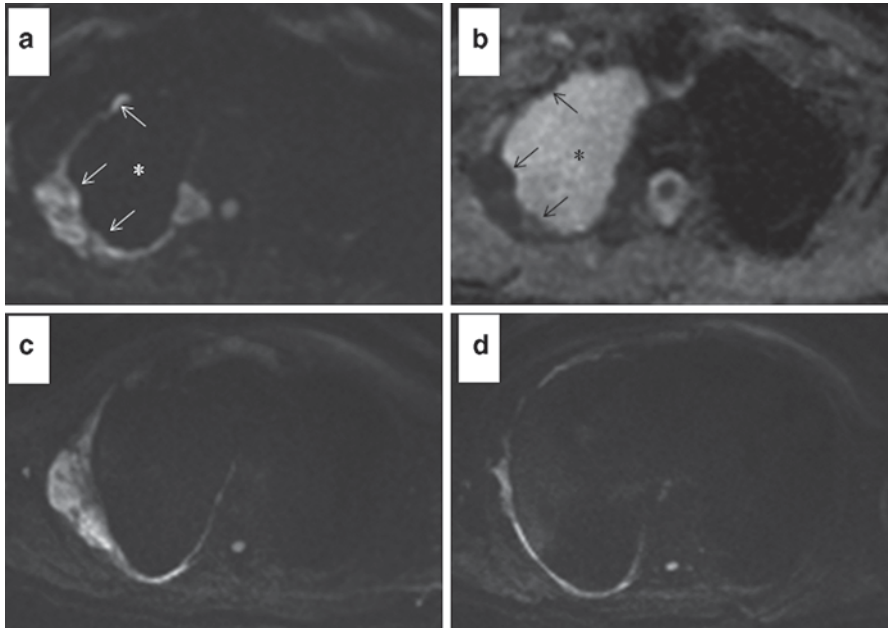
Fig. 3.12 Diffusion-weighted image acquired at b = 800 s/mm^2 (**a**) demonstrates restricted diffusion of the nodular pleural thickening on the right (*arrows*). This finding corresponds to areas of decreased signal on the apparent diffusion coefficient map (**b**). Notice that the signal from the known right pleural effusion (*) has been suppressed on the diffusion-weighted image (**a**) and there is no corresponding low signal on the apparent diffusion coefficient map (**b**). Two additional axial diffusion-weighted images at different locations (**c–d**) demonstrate the rind of restricted diffusion involving the pleura on the right

Ultrasonography

Ultrasonography is a useful technique particularly for targeted evaluation of the pleura. When a pleural effusion is present, it provides an acoustic window which can improve characterization of pleural and even lung findings. Ultrasound-guided thoracenteses as well as percutaneous or transthoracic ultrasound-guided biopsies of pleural masses or thickening are established safe techniques. Ultrasonographic guidance is as effective as CT guidance for transthoracic biopsies with histologic diagnoses achieving greater than 90 % accuracy [83, 84].

Radiological Differential Diagnoses

Many papers have investigated distinguishing between malignant and benign pleural diseases radiologically and although there are a few features that are more suggestive of malignancy, there are a host of other pleural processes besides malig-
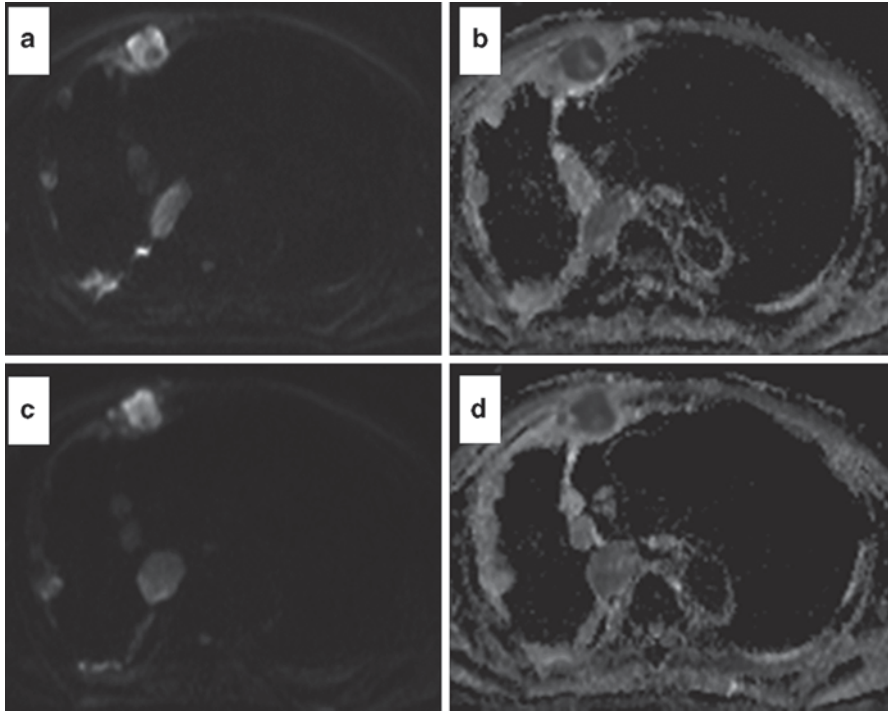
Fig. 3.13 Axial diffusion-weighted imaging and apparent diffusion-coefficient imaging pairs (**a**, **b** and **c**, **d**) at two different locations demonstrate nodular right pleural thickening with focal areas of restricted diffusion. These focal areas of restricted diffusion illustrate the pointillism sign and are suggestive of multifocal deposits of disease

nant pleural mesothelioma which should be on the differential diagnoses. These include but are not limited to solid pleural metastases, fibrous tumor of the pleura, asbestos-related diffuse pleural thickening, pleural fibrosis, and invasive thymoma. Other entities that are lower on the differential list include rounded atelectasis, and pleurodesis.

Cases to Illustrate Radiologic and Clinical Features

Case 1

A 74-year-old man presented with recurrent symptomatic right pleural effusion associated with significant right-sided chest pain and dyspnea. He was a never smoker with possible prior exposure to asbestos when he served in the military several decades ago. A CT obtained to assess for coronary artery calcifications showed a small right pleural effusion in addition to coronary artery calcifications (Fig. 3.15a, b). A
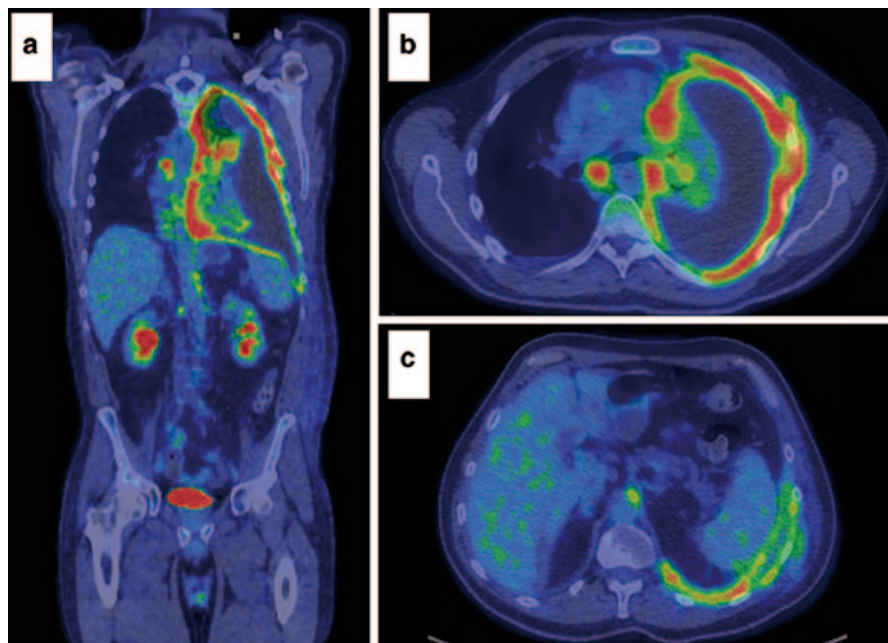
Fig. 3.14 Coronal PET/CT (**a**) and two axial slices (**b**, **c**) show extensive markedly FDG-avid nodular left pleural thickening encasing the left lung. Also seen on PET are FDG-avid right hilar, right infrahilar, and subcarinal lymph nodes indicating contralateral thoracic spread of disease, as well as FDG-avid upper retroperitoneal and right para-aortic lymph nodes consistent with nodal metastases below the diaphragm. A large left pleural effusion is associated with complete collapse of the left lung and resulting mediastinal shift to the right. *FDG* fluorodeoxyglucose, *PET/CT* positron emission tomography/computer tomography
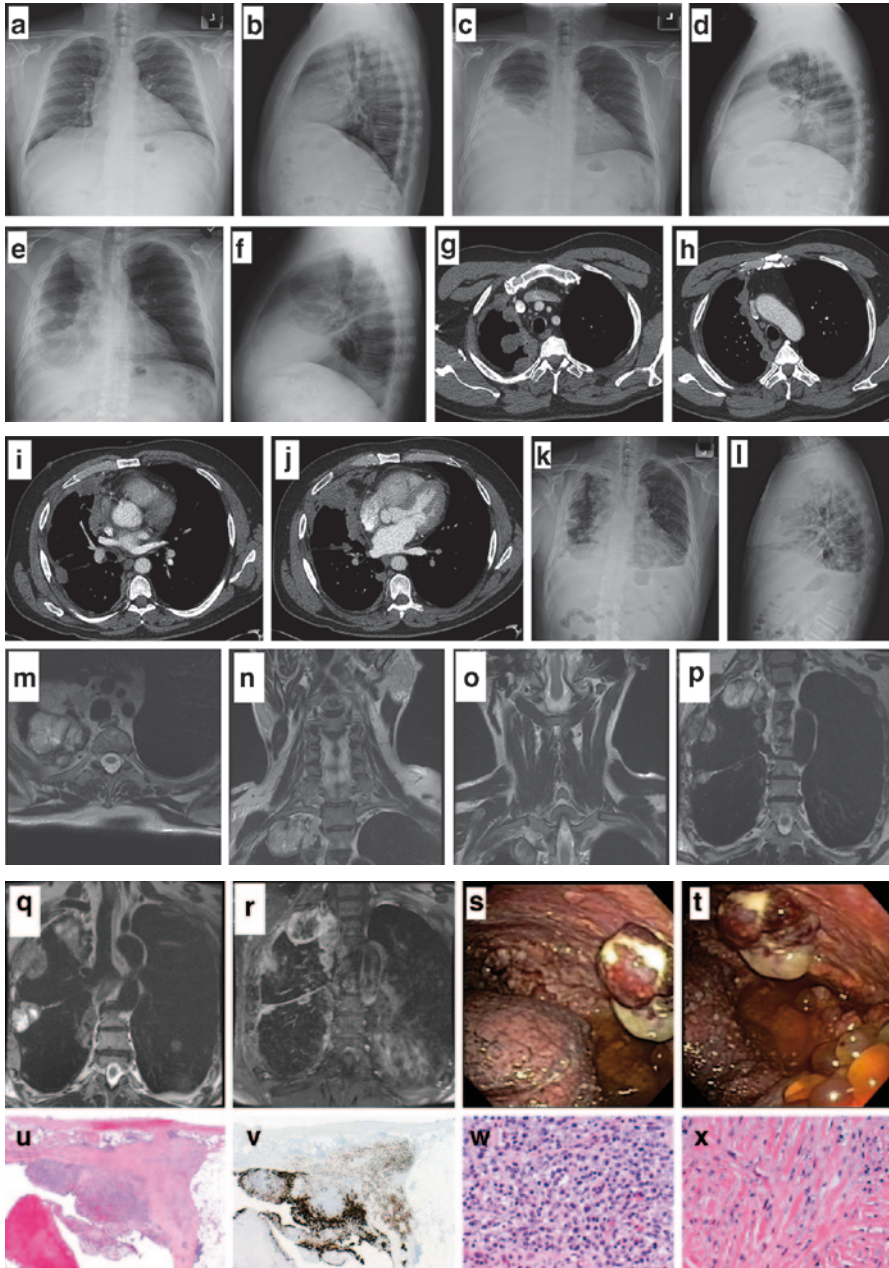
chest radiograph about a year later demonstrated increase in the right pleural effusion and CT showed increased pleural nodularity (Fig. 3.15c–f). The patient subsequently underwent thoracentesis and cytology demonstrated atypical cells. About 1 month later, PET/CT (Fig. 3.15g, h) was obtained and pleuroscopy was performed (Fig. 3.15i, j) with biopsy. The morphologic and immunophenotypic features were consistent with malignant mesothelioma, epithelioid type (Fig. 3.15k, l). The patient expired 25 days later, about 2.5 years after the initial CT.

Case 2

A 59-year-old man presented with a positive TB skin test during a general medical examination. He has no current symptoms and chest radiograph (Fig. 3.16a, b) was normal. One year later, the patient presented with a new right pleural effusion (Fig. 3.16c, d). Nine months later, right pleural masses are identified on follow-up chest radiographs (Fig. 3.16e, f). A CT was obtained (Fig. 3.16g–j) and the diagnosis
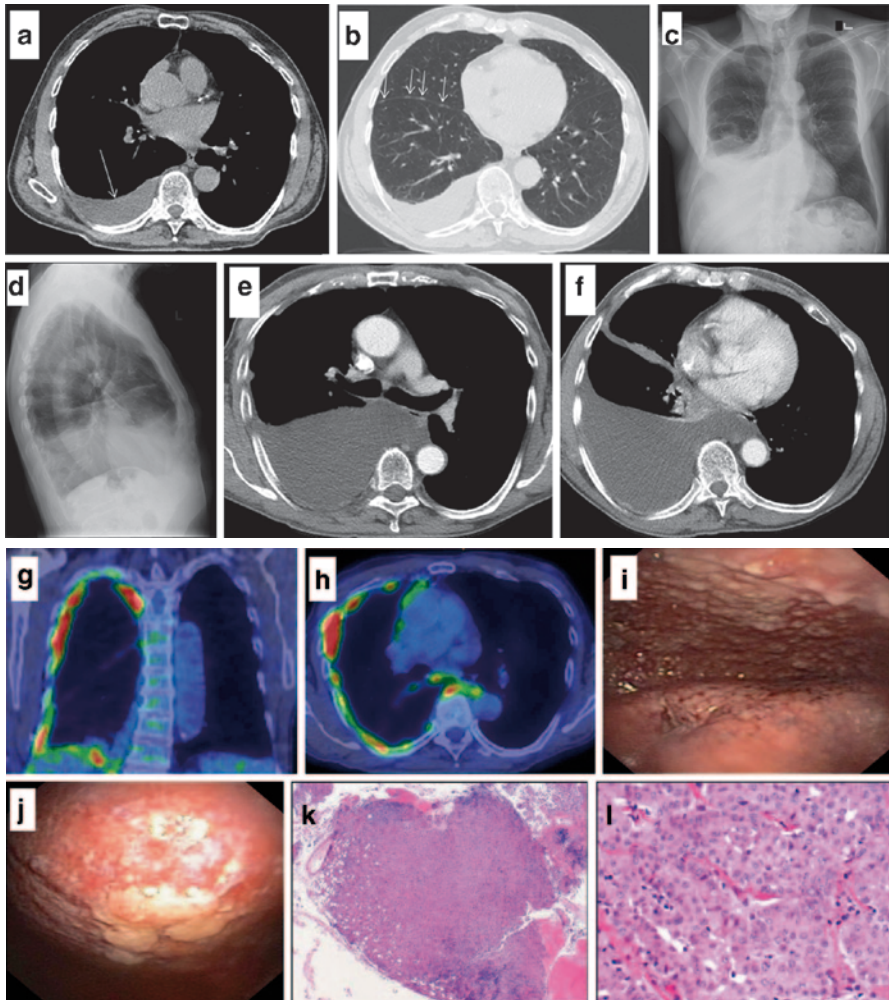
Fig. 3.15 CT without intravenous contrast demonstrates a small right pleural effusion (**a**, *arrow*) and small nodularities (**b**, *arrows*) along the major fissure. Chest radiographs PA (**c**) and lateral (**d**) show an increase in the right pleural effusion and CT (**e**, **f**) demonstrates an increase in the right pleural effusion and increasing pleural nodularity. PET/CT showed extensive nodular hypermetabolic activity involving most of the right pleura (**g**, **h**). Pleuroscopic images (**i**, **j**) demonstrate diffuse nodularity involving the entirety of the parietal pleura. Evaluation also revealed involvement of focal aspects of the visceral pleura, as well as the involvement of the diaphragmatic and mediastinal pleura. Low power view of an H&E slide from a right pleural biopsy reveals sheets of atypical epithelioid cells invading into adipose tissue (**k**). These atypical cells are characterized by ample eosinophilic cytoplasm and round nuclei with prominent nucleoli (**l**). (Magnification x 40 [k], x 400 [l]. The neoplastic cells are positive for calretinin, CK5/6, and WT-1 and lack staining for TTF-1, MOC-31, and BerEp4 (not shown). The morphologic features and immunophenotype are diagnostic of malignant mesothelioma, epithelioid type. *PET/CT* positron emission tomography/computer tomography. (I&J: Courtesy of Dr. John J. Mullon, Mayo Clinic Rochester, MN)

Fig. 3.16 At the time of the positive TB skin test of this 58-year-old man, PA (**a**) and lateral (**b**) chest radiographs were normal. One year later, the patient complained about a cough. Chest radiographs at that time (**c**, **d**) demonstrated a new moderate to large right pleural effusion with associated atelectasis and consolidation of the right mid and lower lung. Chest radiographs 9 months later demonstrated right pleural masses (**e**, **f**). Note their development from the prior two chest radiographs. Contrast-enhanced CT (**g**–**j**) shows circumferential lobulated right pleural thickening

of malignant pleural mesothelioma was established. Chest radiographs (Fig. 3.16k, l) 6 months later showed progression of disease. An MRI of the cervical and thoracic spines (Fig. 3.16m–r) obtained around the same time provided additional characterization of the pleural disease. Pleuroscopy was performed (Fig. 3.16s, t). A biopsy of the parietal pleura revealed biphasic malignant mesothelioma and histopathology (Fig. 3.16u–x) is also shown. Soon after the MRI, about 1.3 years after the right pleural effusion was seen on chest radiograph, the patient expired.

Case 3

A 58-year-old man with a remote smoking history presented with a pulling and pressure sensation deep in the left side of his chest. He has been exposed to various heavy metals from a power plant and possibly has been exposed to asbestos. A chest radiograph (Fig. 3.17a) and PET/CT (Fig. 3.17b, c) were obtained, and a chest CT further characterized the findings (Fig. 3.17d–f). Pleuroscopy was performed (Fig. 3.17g, h) and the diagnosis of malignant mesothelioma was made on a biopsy of the parietal pleura. Later, ultrasonography was obtained for left-sided pleural effusion (Fig. 3.17i, j). A subsequent PET/CT (Fig. 3.17k, l) demonstrated progression of malignant pleural mesothelioma. The patient expired 6 months from the time of the initial chest radiograph.

---

with fissural involvement. No rib erosion is seen. Chest radiographs 6 months later (**k**, **l**) show extensive nodular right pleural thickening, multiple bilateral pulmonary nodules, and a new left pleural effusion. MRI of the cervical and thoracic spine was obtained around the same time and axial (**m**), and coronal (**n**, **o**) nonfat-suppressed T2-weighted images demonstrate right pleural masses and nodular thickening of the pleura. Coronal nonfat-suppressed T2-weighted images (**p**, **q**) show extension into the endothoracic fascia with involvement of the overlying ribs. There is also fissural pleural nodularity. These pleural masses demonstrate heterogeneous enhancement after the administration of intravenous gadolinium-based contrast agent (**r**). Pleuroscopic images show diffuse nodular infiltration of the parietal, diaphragmatic, and to a lesser extent, visceral pleura consistent with the diffuse malignant disease (**s**, **t**). Biopsies from the right parietal pleura reveal sheets of atypical cells growing in a tumefactive pattern and invading into adipose tissue (**u**) as also highlighted by an OSCAR keratin immunostain (**v**). The histologic features are suggestive of a biphasic neoplasm with an epithelioid (**w**) and a sarcomatoid (**x**) component. The tumor cells are focally positive for CK5/6, WT-1 and calretinin and lacked staining for TTF-1, napsin, and MOC31 (not shown). The morphologic and immunophenotypical features are consistent with malignant mesothelioma, biphasic type. Magnification ×40 (**u**, **v**), ×400 (**w**, **x**).(S&T: Courtesy of Dr. Fabien Maldonado, Mayo Clinic Rochester, MN)
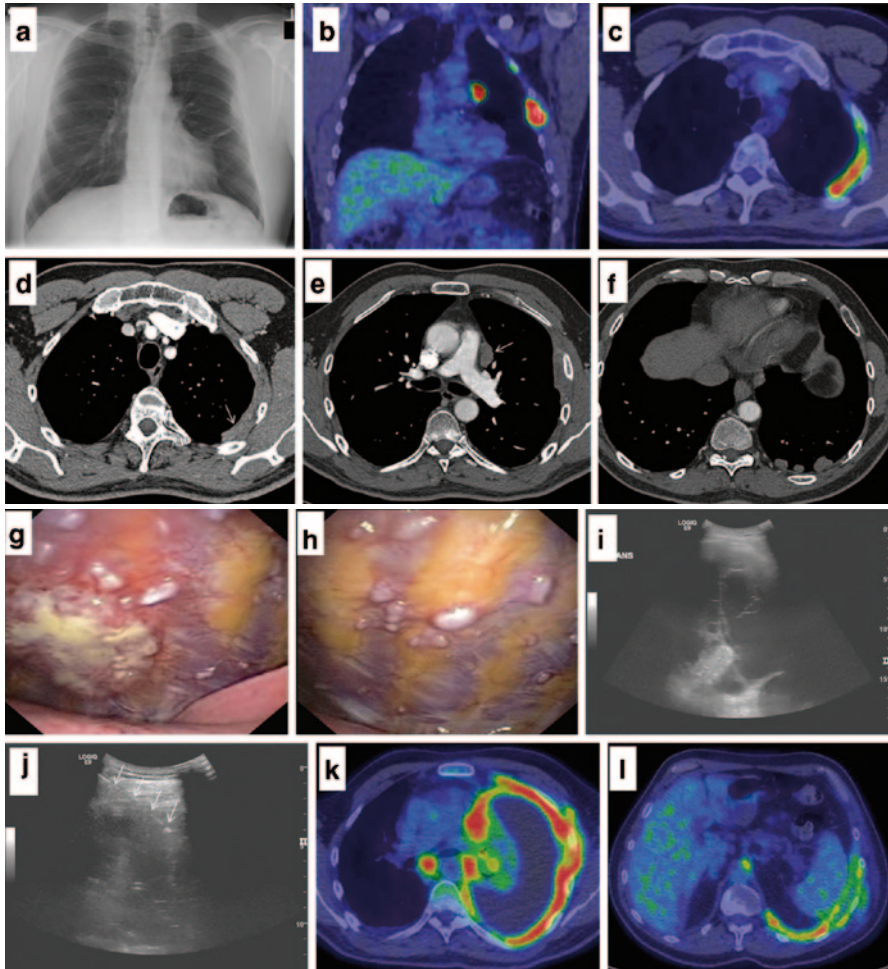
Fig. 3.17 PA chest radiograph (**a**) demonstrats pleural thickening and nodularity about the left lung concerning for metastases or mesothelioma. PET/CT (**b**) shows nodular areas of increased FDG uptake involving the pleura of the left hemithorax both laterally and medially. There are additional areas of hypermetabolic pleural thickening (**c**) on the left. Contrast-enhanced CT of the chest demonstrates plaque-like pleural thickening (*arrow*; **d**), nodules along the mediastinal surface (*arrow*; **e**), and nodules along the left lung base (**f**). Pleuroscopic images (**g**, **h**) demonstrate areas of dense nodularity consistent with pleural plaque and areas of superimposed soft tissue nodularity consistent with malignancy. Ultrasonography show a moderate to large left pleural effusion with atelectasis of the lung (**i**). An ultrasound-guided thoracentesis (**j**) was performed and the catheter (*arrows*) can be seen traversing thickened pleura. PET/CT (**k**, **l**) obtained around the same time demonstrate extensive nodular left pleural thickening which has markedly progressed and causes circumferential encasement of the entire left lung. There is also subcarinal lymphadenopathy. (*FDG* fluorodeoxyglucose, *PET/CT* positron emission tomography/computer tomography). (G&H: Courtesy of Dr. Fabien Maldonado, Mayo Clinic Rochester, MN)

References

1. Robinson BW, Musk AW, Lake RA. Malignant mesothelioma. Lancet. 2005;366:397–408.
2. Ismail-Khan R, Robinson LA, Williams CC Jr, Garrett CR, Bepler G, Simon GR. Malignant pleural mesothelioma: a comprehensive review. Cancer Control. 2006;13:255–63.
3. van Meerbeeck JP, Scherpereel A, Surmont VF, Baas P. Malignant pleural mesothelioma: the standard of care and challenges for future management. Crit Rev Oncol Hematol. 2011;78:92–111.
4. Sheard JD, Taylor W, Soorae A, Pearson MG. Pneumothorax and malignant mesothelioma in patients over the age of 40. Thorax. 1991;46:584–5.
5. Alkhuja S, Miller A, Mastellone AJ, Markowitz S. Malignant pleural mesothelioma presenting as spontaneous pneumothorax: a case series and review. Am J Ind Med. 2000;38:219–23.
6. Seely JM, Nguyen ET, Churg AM, Muller NL. Malignant pleural mesothelioma: computed tomography and correlation with histology. Eur J Radiol. 2009;70:485–91.
7. Adams VI, Unni KK, Muhm JR, Jett JR, Ilstrup DM, Bernatz PE. Diffuse malignant mesothelioma of pleura. Diagnosis and survival in 92 cases. Cancer. 1986;58:1540–51.
8. British Thoracic Society Standards of Care Committee. BTS statement on malignant mesothelioma in the UK, 2007. Thorax 2007;62(Suppl 2):ii1–19.
9. Larsen BT, Klein JR, Hornychova H, et al. Diffuse intrapulmonary malignant mesothelioma masquerading as interstitial lung disease: a distinctive variant of mesothelioma. Am J Surg Pathol. 2013;37:1555–64.
10. Rossi G, Cavazza A, Turrini E, et al. Exclusive intrapulmonary lepidic growth of a malignant pleural mesothelioma presenting with pneumothorax and involving the peritoneum. Int J Surg Pathol. 2006;14:234–7.
11. Heki U, Fujimura M, Kasahara K, Matsubara F, Matsuda T. Malignant mesothelioma presenting as pulmonary metastasis ahead of growth of primary tumour. Respirology. 1999;4:279–81.
12. Musk AW, Dewar J, Shilkin KB, Whitaker D. Miliary spread of malignant pleural mesothelioma without a clinically identifiable pleural tumour. Aust NZ J Med. 1991;21:460–2.
13. Nind NR, Attanoos RL, Gibbs AR. Unusual intraparenchymal growth patterns of malignant pleural mesothelioma. Histopathology. 2003;42:150–5.
14. Gunday M, Erinanc H, Geredeli C. Unusual region for pericardial malignant mesothelioma: cutaneous manifestation in a Turkish woman. Rare Tumors. 2013;5:e41.
15. Wild K, Sankaran P, Nagy A, Sington J. Meningeal and brainstem infiltration by a malignant mesothelioma. BMJ Case Rep. 2010.
16. Elbahaie AM, Kamel DE, Lawrence J, Davidson NG. Late cutaneous metastases to the face from malignant pleural mesothelioma: a case report and review of the literature. World J Surg Oncol. 2009;7:84.
17. Sussman J, Rosai J. Lymph node metastasis as the initial manifestation of malignant mesothelioma. Report of six cases. Am J Surg Pathol. 1990;14:819–28.
18. Yakirevich E, Sova Y, Drumea K, Bergman I, Quitt M, Resnick MB. Peripheral lymphadenopathy as the initial manifestation of pericardial mesothelioma: a case report. Int J Surg Pathol. 2004;12:403–5.
19. Craig FE, Fishback NF, Schwartz JG, Powers CN. Occult metastatic mesothelioma–diagnosis by fine-needle aspiration. A case report. Am J Clin Pathol. 1992;97:493–7.
20. Zhang Y, Taheri ZM, Jorda M. Systemic lymphadenopathy as the initial presentation of malignant mesothelioma: a report of three cases. Patholog Res Int. 2010;2010:846571.
21. Lloreta J, Serrano S. Pleural mesothelioma presenting as an axillary lymph node metastasis with anemone cell appearance. Ultrastruct Pathol. 1994;18:293–8.
22. Wills EJ. Pleural mesothelioma with initial presentation as cervical lymphadenopathy. Ultrastruct Pathol. 1995;19:389–94.
23. Tammilehto L, Maasilta P, Kostiainen S, Appelqvist P, Holsti LR, Mattson K. Diagnosis and prognostic factors in malignant pleural mesothelioma: a retrospective analysis of sixty-five patients. Respiration. 1992;59:129–35.

24. Tanrikulu AC, Abakay A, Kaplan MA, et al. A clinical, radiographic and laboratory evaluation of prognostic factors in 363 patients with malignant pleural mesothelioma. Respiration. 2010;80:480–7.
25. Yates DH, Corrin B, Stidolph PN, Browne K. Malignant mesothelioma in south east England: clinicopathological experience of 272 cases. Thorax. 1997;52:507–12.
26. Bani-Hani KE, Gharaibeh KA. Malignant peritoneal mesothelioma. J Surg Oncol. 2005;91:17–25.
27. Bridda A, Padoan I, Mencarelli R, Frego M. Peritoneal mesothelioma: a review. Med Gen Med. 2007;9:32.
28. Eltabbakh GH, Piver MS, Hempling RE, Recio FO, Intengen ME. Clinical picture, response to therapy, and survival of women with diffuse malignant peritoneal mesothelioma. J Surg Oncol. 1999;70:6–12.
29. Asensio JA, Goldblatt P, Thomford NR. Primary malignant peritoneal mesothelioma. A report of seven cases and a review of the literature. Arch Surg. 1990;125:1477–81.
30. Acherman YI, Welch LS, Bromley CM, Sugarbaker PH. Clinical presentation of peritoneal mesothelioma. Tumori. 2003;89:269–73.
31. Ribak J, Lilis R, Suzuki Y, Penner L, Selikoff IJ. Malignant mesothelioma in a cohort of asbestos insulation workers: clinical presentation, diagnosis, and causes of death. Br J Ind Med. 1988;45:182–7.
32. Salemis NS, Tsiambas E, Gourgiotis S, Mela A, Karameris A, Tsohataridis E. Peritoneal mesothelioma presenting as an acute surgical abdomen due to jejunal perforation. J Dig Dis. 2007;8:216–21.
33. Yan TD, Popa E, Brun EA, Cerruto CA, Sugarbaker PH. Sex difference in diffuse malignant peritoneal mesothelioma. Br J Surg. 2006;93:1536–42.
34. Mani H, Merino MJ. Mesothelial neoplasms presenting as, and mimicking, ovarian cancer. Int J Gynecol Pathol. 2010;29:523–8.
35. Baker PM, Clement PB, Young RH. Malignant peritoneal mesothelioma in women: a study of 75 cases with emphasis on their morphologic spectrum and differential diagnosis. Am J Clin Pathol. 2005;123:724–37.
36. Manzini VP, Recchia L, Cafferata M, et al. Malignant peritoneal mesothelioma: a multicenter study on 81 cases. Ann Oncol. 2010;21:348–53.
37. Schneiderman H. Mesothelioma and venous thrombosis. CMAJ. 2004;171:11, author reply -2.
38. Banayan S, Hot A, Janier M, Ninet J, Zurlinden O, Billotey C. Malignant mesothelioma of the peritoneum as the cause of a paraneoplastic syndrome: detection by 18F-FDG PET. Eur J Nucl Med Mol Imaging. 2006;33:751.
39. Socola F, Loaiza-Bonilla A, Bustinza-Linares E, Correa R, Rosenblatt JD. Recurrent thrombotic thrombocytopenic purpura-like syndrome as a paraneoplastic phenomenon in malignant peritoneal mesothelioma: a case report and review of the literature. Case Rep Oncol Med. 2012;2012:619348.
40. Bech C, Sorensen JB. Polyneuropathy in a patient with malignant pleural mesothelioma: a paraneoplastic syndrome. J Thorac Oncol. 2008;3:1359–60.
41. Archer HA, Panopoulou A, Bhatt N, Edey AJ, Giffin NJ. Mesothelioma and anti-Ma paraneoplastic syndrome; heterogeneity in immunogenic tumours increases. Pract Neurol. 2014;14(1):33–5.
42. Tanriverdi O, Meydan N, Barutca S, Ozsan N, Gurel D, Veral A. Anti-Yo antibody-mediated paraneoplastic cerebellar degeneration in a female patient with pleural malignant mesothelioma. Jpn J Clin Oncol. 2013;43:563–8.
43. Britton M. The epidemiology of mesothelioma. Semin Oncol. 2002;29:18–25.
44. Jarvholm B, Sanden A. Lung cancer and mesothelioma in the pleura and peritoneum among Swedish insulation workers. Occup Environ Med. 1998;55:766–70.
45. Hilliard AK, Lovett JK, McGavin CR. The rise and fall in incidence of malignant mesothelioma from a British Naval Dockyard, 1979–1999. Occup Med (Lond). 2003;53:209–12.

46. Abakay A, Tanrikulu AC, Kaplan MA, et al. Clinical characteristics and treatment outcomes in 132 patients with malignant mesothelioma. Lung India. 2011;28:267–71.
47. Antman KH, Blum RH, Greenberger JS, Flowerdew G, Skarin AT, Canellos GP. Multimodality therapy for malignant mesothelioma based on a study of natural history. Am J Med. 1980;68:356–62.
48. Rosas-Salazar C, Gunawardena SW, Spahr JE. Malignant pleural mesothelioma in a child with ataxia-telangiectasia. Pediatr Pulmonol. 2013;48:94–7.
49. Fraire AE, Cooper S, Greenberg SD, Buffler P, Langston C. Mesothelioma of childhood. Cancer. 1988;62:838–47.
50. Moran CA, Albores-Saavedra J, Suster S. Primary peritoneal mesotheliomas in children: a clinicopathological and immunohistochemical study of eight cases. Histopathology. 2008;52:824–30.
51. Light RW, Macgregor MI, Luchsinger PC, Ball WC Jr. Pleural effusions: the diagnostic separation of transudates and exudates. Ann Intern Med. 1972;77:507–13.
52. Gottehrer A, Taryle DA, Reed CE, Sahn SA. Pleural fluid analysis in malignant mesothelioma. Prognostic implications. Chest. 1991;100:1003–6.
53. Pass HI, Levin SM, Harbut MR, et al. Fibulin-3 as a blood and effusion biomarker for pleural mesothelioma. N Engl J Med. 2012;367:1417–27.
54. Campbell NP, Kindler HL. Update on malignant pleural mesothelioma. Semin Respir Crit Care Med. 2011;32:102–10.
55. Pass HI, Lott D, Lonardo F, et al. Asbestos exposure, pleural mesothelioma, and serum osteopontin levels. N Engl J Med. 2005;353:1564–73.
56. Shi HZ, Liang QL, Jiang J, Qin XJ, Yang HB. Diagnostic value of carcinoembryonic antigen in malignant pleural effusion: a meta-analysis. Respirology. 2008;13:518–27.
57. Grigoriu BD, Grigoriu C, Chahine B, Gey T, Scherpereel A. Clinical utility of diagnostic markers for malignant pleural mesothelioma. Monaldi Arch Chest Dis. 2009;71:31–8.
58. Fuhrman C, Duche JC, Chouaid C, et al. Use of tumor markers for differential diagnosis of mesothelioma and secondary pleural malignancies. Clin Biochem. 2000;33:405–10.
59. Frebourg T, Lerebours G, Delpech B, et al. Serum hyaluronate in malignant pleural mesothelioma. Cancer. 1987;59:2104–7.
60. Chiu B, Churg A, Tengblad A, Pearce R, McCaughey WT. Analysis of hyaluronic acid in the diagnosis of malignant mesothelioma. Cancer. 1984;54:2195–9.
61. Creaney J, Dick IM, Segal A, Musk AW, Robinson BW. Pleural effusion hyaluronic acid as a prognostic marker in pleural malignant mesothelioma. Lung Cancer. 2013;82:491–8.
62. Filiberti R, Parodi S, Libener R, et al. Diagnostic value of mesothelin in pleural fluids: comparison with CYFRA 21-1 and CEA. Med Oncol. 2013;30:543.
63. O'Rahilly R, Muller NL, Carpenter S, Swenson R. Basic human anatomy: A regional study of human structure. Chapter 22. In: O'Rahilly R, editor. Online version. Dartmouth Medical School and Dartmouth College, New Hampshire, USA; 2008.
64. Gray H, editor. Anatomy of the human body. New York: Bartleby.com; 2000.
65. Rusch VW. A proposed new international TNM staging system for malignant pleural mesothelioma from the International Mesothelioma Interest Group. Lung Cancer. 1996;14:1–12.
66. Rusch VW, Giroux D. Do we need a revised staging system for malignant pleural mesothelioma? Analysis of the IASLC database. Ann Cardiothorac Surg. 2012;1:438–48.
67. Rusch VW, Giroux D, Kennedy C, et al. Initial analysis of the international association for the study of lung cancer mesothelioma database. J Thorac Oncol. 2012;7:1631–9.
68. Kawashima A, Libshitz HI. Malignant pleural mesothelioma: CT manifestations in 50 cases. AJR Am J Roentgenol. 1990;155:965–9.
69. Metintas M, Ucgun I, Elbek O, et al. Computed tomography features in malignant pleural mesothelioma and other commonly seen pleural diseases. Eur J Radiol. 2002;41:1–9.
70. Armato SG 3rd, Labby ZE, Coolen J, et al. Imaging in pleural mesothelioma: a review of the 11th International Conference of the International Mesothelioma Interest Group. Lung Cancer. 2013;82:190–6.

71. Corson N, Sensakovic WF, Straus C, Starkey A, Armato SG 3rd. Characterization of mesothe-lioma and tissues present in contrast-enhanced thoracic CT scans. Med Phys. 2011;38:942–7.
72. Patz EF Jr, Shaffer K, Piwnica-Worms DR, et al. Malignant pleural mesothelioma: value of CT and MR imaging in predicting resectability. AJR Am J Roentgenol. 1992;159:961–6.
73. Heelan RT, Rusch VW, Begg CB, Panicek DM, Caravelli JF, Eisen C. Staging of malig-nant pleural mesothelioma: comparison of CT and MR imaging. AJR Am J Roentgenol. 1999;172:1039–47.
74. Coolen J, De Keyzer F, Nafteux P, et al. Malignant pleural disease: diagnosis by using dif-fusion-weighted and dynamic contrast-enhanced MR imaging–initial experience. Radiology. 2012;263:884–92.
75. Byrne MJ, Nowak AK. Modified RECIST criteria for assessment of response in malignant pleural mesothelioma. Ann Oncol. 2004;15:257–60.
76. Sensakovic WF, Armato SG 3rd, Starkey A, Kindler HL, Vigneswaran WT. Quantitative measurement of lung reexpansion in malignant pleural mesothelioma patients undergoing pleurectomy/decortication. Acad Radiol. 2011;18:294–8.
77. Flores RM. The role of PET in the surgical management of malignant pleural mesothelioma. Lung Cancer. 2005;49(Suppl 1):S27–32.
78. Flores RM, Akhurst T, Gonen M, Larson SM, Rusch VW. Positron emission tomography defines metastatic disease but not locoregional disease in patients with malignant pleural mesothelioma. J Thorac Cardiovasc Surg. 2003;126:11–6.
79. Truong MT, Viswanathan C, Godoy MB, Carter BW, Marom EM. Malignant pleural meso-thelioma: role of CT, MRI, and PET/CT in staging evaluation and treatment considerations. Semin Roentgenol. 2013;48:323–34.
80. Duysinx B, Nguyen D, Louis R, et al. Evaluation of pleural disease with 18-fluorodeoxyglu-cose positron emission tomography imaging. Chest. 2004;125:489–93.
81. Kinahan PE, Fletcher JW. Positron emission tomography-computed tomography standard-ized uptake values in clinical practice and assessing response to therapy. Semin Ultrasound CT MR. 2010;31:496–505.
82. Margolis DJ, Hoffman JM, Herfkens RJ, Jeffrey RB, Quon A, Gambhir SS. Molecular imag-ing techniques in body imaging. Radiology. 2007;245:333–56.
83. Jeon KN, Bae K, Park MJ, et al. US-guided transthoracic biopsy of peripheral lung lesions: pleural contact length influences diagnostic yield. Acta Radiol. 2014;55(3):295–301.
84. Yang PC. Ultrasound-guided transthoracic biopsy of peripheral lung, pleural, and chest-wall lesions. J Thorac Imaging. 1997;12:272–84.
85. Law MR, Hodson ME, Turner-Warwick M. Malignant mesothelioma of the pleura: clinical aspects and symptomatic treatment. Eur J Respir Dis. 1984;65:162–8.